

Research Article

PKC isoforms activate LRRK1 kinase by phosphorylating conserved residues (Ser1064, Ser1074 and Thr1075) within the COR_B GTPase domain

Asad U. Malik^{1,2,*}, Athanasios Karapetsas^{1,*}, Raja S. Nirujogi^{1,2}, Deep Chatterjee^{2,3}, Toan K. Phung^{1,2}, Melanie Wightman¹, Robert Gourlay¹, Nick Morrice⁴,  Sebastian Mathea^{2,3}, Stefan Knapp^{2,3} and  Dario R. Alessi^{1,2}

¹Medical Research Council (MRC) Protein Phosphorylation and Ubiquitylation Unit, School of Life Sciences, University of Dundee, Dow Street, Dundee DD1 5EH, U.K.; ²Aligning Science Across Parkinson's (ASAP) Collaborative Research Network, Chevy Chase, MD 20815, U.S.A.; ³Structural Genomics Consortium, Buchmann Institute for Molecular Life Sciences and Institute for Pharmaceutical Chemistry, Johann Wolfgang Goethe-University, Max-von-Laue-Str. 9, D-60438 Frankfurt am Main, Germany; ⁴AB Sciex, Alderley Park, Macclesfield SK10 4TG, U.K.

Correspondence: Dario R. Alessi (d.r.alessi@dundee.ac.uk)



Leucine-rich-repeat-kinase 1 (LRRK1) and its homolog LRRK2 are multidomain kinases possessing a ROC-COR_A-COR_B containing GTPase domain and phosphorylate distinct Rab proteins. LRRK1 loss of function mutations cause the bone disorder osteosclerotic metaphyseal dysplasia, whereas LRRK2 missense mutations that enhance kinase activity cause Parkinson's disease. Previous work suggested that LRRK1 but not LRRK2, is activated via a Protein Kinase C (PKC)-dependent mechanism. Here we demonstrate that phosphorylation and activation of LRRK1 in HEK293 cells is blocked by PKC inhibitors including LXS-196 (Darovasertib), a compound that has entered clinical trials. We show multiple PKC isoforms phosphorylate and activate recombinant LRRK1 in a manner reversed by phosphatase treatment. PKC α unexpectedly does not activate LRRK1 by phosphorylating the kinase domain, but instead phosphorylates a cluster of conserved residues (Ser1064, Ser1074 and Thr1075) located within a region of the COR_B domain of the GTPase domain. These residues are positioned at the equivalent region of the LRRK2 DK helix reported to stabilize the kinase domain α C-helix in the active conformation. Thr1075 represents an optimal PKC site phosphorylation motif and its mutation to Ala, blocked PKC-mediated activation of LRRK1. A triple Glu mutation of Ser1064/Ser1074/Thr1075 to mimic phosphorylation, enhanced LRRK1 kinase activity ~3-fold. From analysis of available structures, we postulate that phosphorylation of Ser1064, Ser1074 and Thr1075 activates LRRK1 by promoting interaction and stabilization of the α C-helix on the kinase domain. This study provides new fundamental insights into the mechanism controlling LRRK1 activity and reveals a novel unexpected activation mechanism.

*These authors contributed equally to this work.

Received: 9 June 2022
Revised: 17 August 2022
Accepted: 30 August 2022

Accepted Manuscript online:
30 August 2022
Version of Record published:
23 September 2022

Introduction

The Leucine Rich Repeat Protein Kinase-1 (LRRK1) and its paralog LRRK2 are large multidomain protein kinases possessing ANK, LRR, ROC-COR_A-COR_B containing ROCO GTPase, kinase and WD40 domains [1]. In addition, LRRK2 possesses an N-terminal ARM domain not-present in LRRK1 [2]. Rare recessive loss of function mutations in LRRK1 lead to a serious bone disorder termed osteosclerotic metaphyseal dysplasia [3,4]. Autosomal dominant mutations that enhance the kinase activity of LRRK2 cause familial late onset Parkinson's that is similar in phenotype to the

idiopathic form of the disease [5,6]. LRRK1 and LRRK2 phosphorylate distinct Rab GTPase proteins within their Switch-II effector binding motif. LRRK1 phosphorylates Rab7A at Ser72 [7,8], whereas LRRK2 phosphorylates a subset of Rab proteins, including Rab8A, Rab10 and Rab12 [9,10]. LRRK2 phosphorylation of Rab proteins does not affect GTPase activity but controls effector binding by promoting interaction with effectors such as RILPL1/RILPL2 [10,11], JIP3/JIP4 [11,12] and myosin-Va [13] that are critical in controlling downstream biology.

Our previous work suggests that LRRK1, but not LRRK2, is stimulated by phorbol esters that switch on conventional and novel PKC isoforms [8]. In contrast, LRRK2 is activated by recruitment to membrane vesicles, through binding to Rab GTPases such as Rab29 that interacts with the ARM domain that is not present in LRRK1 [14–18]. Furthermore, a Parkinson's causing mutation in VPS35[D620N] stimulates LRRK2 activity without impacting LRRK1 [8,19]. Thus, although LRRK1 and LRRK2 are close homologs, mutations in these two kinases have been linked to the development of diverse diseases, they are stimulated by distinct pathways and phosphorylate different Rab substrates (Table 1).

There are multiple isoforms of PKC belonging to the larger family of AGC protein kinases [20,21]. Many AGC kinases including all PKC isoforms are activated by T-loop phosphorylation by the 3-phosphoinositide dependent protein kinase-1 (PDK1) [22,23]. Activity of conventional and novel PKC isoforms is also regulated by phosphorylation of their hydrophobic motif residue that recent work suggests is controlled by autophosphorylation via the mTORC2 kinase phosphorylating the TOR Interacting motif [24]. Conventional (PKC α , PKC β , PKC γ) and novel (PKC δ , PKC ϵ , PKC η and PKC θ) PKC isoforms are stimulated by lipids such as diacylglycerol though only conventional isoforms also bind and are activated by Ca²⁺ [25]. Phorbol esters are substances from plants that mimic the function of diacylglycerol. They are widely used tools to activate PKCs in cell-culture experiments. The atypical PKCs (PKC ι and PKC ζ) are regulated by a distinct upstream pathway but still require PDK1 to be activated [26–28]. PKC isoforms phosphorylate a multitude of substrates involved in regulating a wide range of cellular pathways. Classical PKC substrates are phosphorylated on a Ser/Thr residue lying in a motif that possess a basic residue at the –3 and –5 positions and a hydrophobic residue at the +1 positions [29], although PKCs can also phosphorylate substrates at non canonical sites deviating from this optimal motif [30].

We previously observed that stimulation of mouse embryonic fibroblasts (MEFs) with phorbol ester, induced marked phosphorylation of Rab7A in a manner that was blocked by knock-out of LRRK1, treatment with a non-specific LRRK1 inhibitor GZD824 or treatment with a relatively non-specific GÖ6983 PKC isoform inhibitor [8]. These results suggested that PKC isoforms play a role in regulating the activation of LRRK1, but the mechanism by which PKC could control LRRK1 remained elusive. In this study, we explored the activation mechanism further and demonstrate that PKC isoforms directly activate LRRK1 by phosphorylating a cluster of highly conserved residues (Ser1064, Ser1074 and Ser1075) located within the COR β domain that forms part of the Roco GTPase domain. Our data provides firm evidence that LRRK1 is a direct downstream target of PKC isoforms. After PKD isoforms that are also activated by PKC isoforms [31], LRRK1 is thus the second class of kinase to be demonstrated to be directly activated by PKC isoforms. It also establishes a new paradigm by which phosphorylation of the COR β located within the GTPase domain can directly stimulate LRRK1 kinase activity.

Results

Establishing a cell system to dissect the mechanism of LRRK1 regulation by PKC isoforms

Consistent with previous findings in MEFs [32], phorbol ester stimulation enhanced Rab7A phosphorylation at Ser72 in control non-transfected HEK293 cells, and to greater extent in HEK293 cells that stably overexpress GFP-LRRK1 (Figure 1A). This was blocked by the PKC inhibitor GÖ6983 (1 μ M) (Figure 1A). Immunoblotting with a pan selective PKC site phospho-specific substrate antibody [33], confirmed phorbol ester triggered phosphorylation of a multitude of cellular proteins which was suppressed by GÖ6983 (Figure 1A). A time course of phorbol ester stimulation revealed that increased Rab7A phosphorylation was detectable within 1 min, plateauing between 20 and 40 min, and declining thereafter, paralleling phosphorylation of ERK1/2 (Figure 1B, quantified in Supplementary Figure S1), that is triggered by PKC activation [34]. PKC α levels decreased ~40% between 80 to 160 min paralleling a similar decline in Rab7A phosphorylation (Figure 1B, quantified in Supplementary Figure S1). Stable expression of kinase inactive LRRK1[D1409A], did

Table 1 Comparing LRRK1 and LRRK2

	LRRK1	LRRK2
Associated disease	Osteosclerotic metaphyseal dysplasia (loss of function mutation) [3, 4]	Parkinson's disease (gain of function/kinase domain activating mutations) [5, 6].
Substrates	Rab7A [7, 8]. LRRK1 does not phosphorylate Rab8A and Rab10, further work needed to investigate other Rab targets	Rab1, Rab3, Rab8, Rab10, Rab12, Rab29, Rab35 and Rab43. [9, 10]. LRRK2 does not phosphorylate Rab7A [8]
Upstream regulation	Phorbol ester or EGF stimulation [8]	<ol style="list-style-type: none"> 1. Recruitment of LRRK2 to membranes by binding to Rab proteins (e.g Rab8A, Rab10 and Rab29 and pRab8A, pRab10) via ARM domain [14, 15, 17]. 2. Parkinson's mutations of the retromer complex [19]. 3. Lysosomal stress/damage candida infection, LLOMe, chloroquine [12, 55, 56] 4. Nigericin and monensin (unknown mechanism) [57]

not increase Rab7A phosphorylation beyond that induced by endogenous LRRK1 following phorbol ester treatment (Figure 1C). Consistent with LRRK2 not being controlled by PKC, phosphorylation of the LRRK2 specific substrate Rab10 at Thr73, was not impacted by phorbol ester stimulation (Figure 1C). Bryostatin-1 a macrocyclic lactone produced by the marine organism *Bugula neritina* that binds to the phorbol ester receptor and activates PKC isoforms [35], also triggered phosphorylation of Rab7A in a manner that was blocked by GÖ6983 (Figure 1D).

Optimizing cell lysis conditions to preserve LRRK1 kinase activity

In performing pilot immunoprecipitation studies, we noted that immunoprecipitated LRRK1 isolated from cell lysates prepared in 1% (v/v) Triton-X100 detergent, displayed low activity when compared with recombinant LRRK1[20-2015] produced in insect cells (Figure 2A). This prompted us to investigate other detergents and we found that the kinase activity of immunoprecipitated LRRK1 activity was significantly higher and closer to the

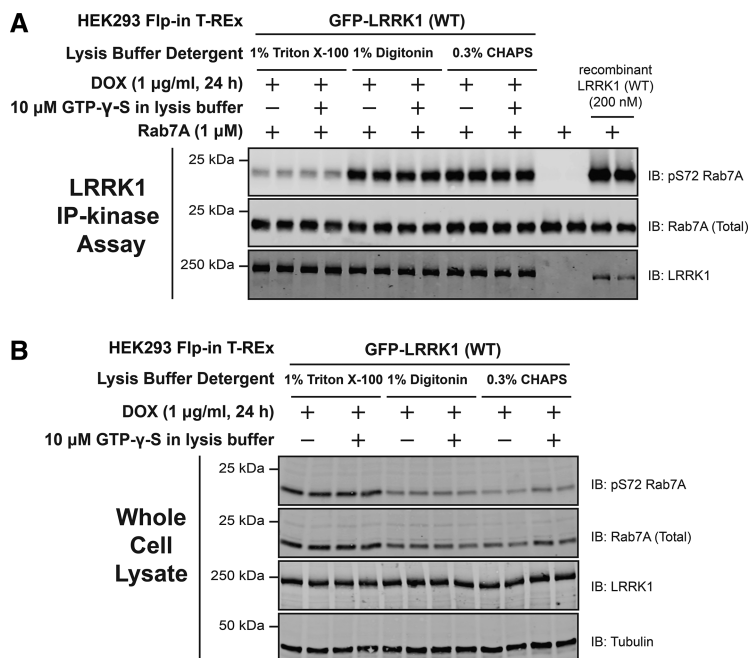


Figure 2. Optimizing cell lysis conditions to preserve LRRK1 kinase activity.

(A) HEK293 Flp-in T-REx cells stably expressing wild type (WT) GFP-LRRK1, were treated with 1 µg/ml doxycycline for 24 h to induce expression of GFP-LRRK1. Cells were harvested in a lysis buffer containing (50 mM HEPES, pH 7.4, 270 mM sucrose, 150 mM NaCl, 1 mM sodium orthovanadate, 50 mM NaF, 10 mM 2- glycerophosphate, 5 mM sodium pyrophosphate, 1 µg/ml microcystin-LR and complete EDTA-free protease inhibitor cocktail) the indicated detergent ± 10 µM GTP-γ-S. GFP-LRRK1 was immunoprecipitated from cell lysates using an anti-GFP nanobody. Immunoprecipitates were washed in the same cell lysis buffer before being washed into kinase assay buffer (25 mM HEPES pH7.4, 50 mM KCl, 0.1% (v/v) 2-mercaptoethanol). LRRK1 kinase activity towards recombinant Rab7A was assessed in a 30 min assay. Reactions were terminated by addition of SDS-sample buffer and levels of pSer72-Rab7A, Rab7A and LRRK1 were assessed by quantitative immunoblot analysis using the LI-COR Odyssey CLx Western Blot imaging system with the indicated antibodies. Combined immunoblotting data from two independent biological replicates (each performed in duplicate) are shown. (B) The whole cell extracts (10 µg) that were prepared in (A) were subjected to quantitative immunoblot analysis using the LI-COR Odyssey CLx Western Blot imaging system with the indicated antibodies.

of immunoprecipitated LRRK1 by ~7.5-fold (Figure 3A). Immunoblotting revealed that phorbol ester increased recognition of immunoprecipitated LRRK1 with a pan-phospho-PKC substrate motif antibody [36], consistent with the notion that PKC directly phosphorylates LRRK1 (Figure 3A). Incubation of cells with increasing doses of the LXS-196 (Darovasertib), a PKC inhibitor, that is currently in human clinical cancer trials [37], and highly specific [38], resulted in a concentration dependent inhibition of immunoprecipitated LRRK1 kinase activity, with an IC₅₀ of ~40 nM (Figure 3A). The inhibition of LRRK1 activity *in vitro* paralleled that of endogenous Rab7A phosphorylation, as well as cellular PKC substrate phosphorylation (Figure 3B). LXS-196 is structurally unrelated to GÖ6983 that is a staurosporine analog and a much less selective kinase inhibitor [39]. The GÖ6983 inhibitor also blocked phorbol ester induced activation of LRRK1 activity (Figure 3B).

PKC isoforms activate PKD kinases [31,40]. To rule out PKD activating LRRK1, we used a PKD kinase inhibitor termed CRT0066051 (1 µM) [41] and found that treating cells with this selective PKD inhibitor did not impact phorbol ester mediated activation of LRRK1 (Figure 3B). CRT0066051 reduced autophosphorylation of PKD1 at Ser910 confirming that inhibitor suppressed kinase PKD1 activity (Figure 3B) [41]. As expected, LXS-196 and GÖ6983 PKC inhibitors also suppressed autophosphorylation of PKD1 at Ser910 (Figure 3B).

We investigated whether the kinase activity of endogenous LRRK1 was similarly stimulated upon phorbol ester treatment. To this end, we employed previously characterized wild type and homozygous LRRK1 knock-out MEFs [8] and stimulated these cells ± phorbol ester. Endogenous LRRK1 was immunoprecipitated and assayed employing recombinant Rab7A as a substrate. This revealed that phorbol ester markedly stimulated

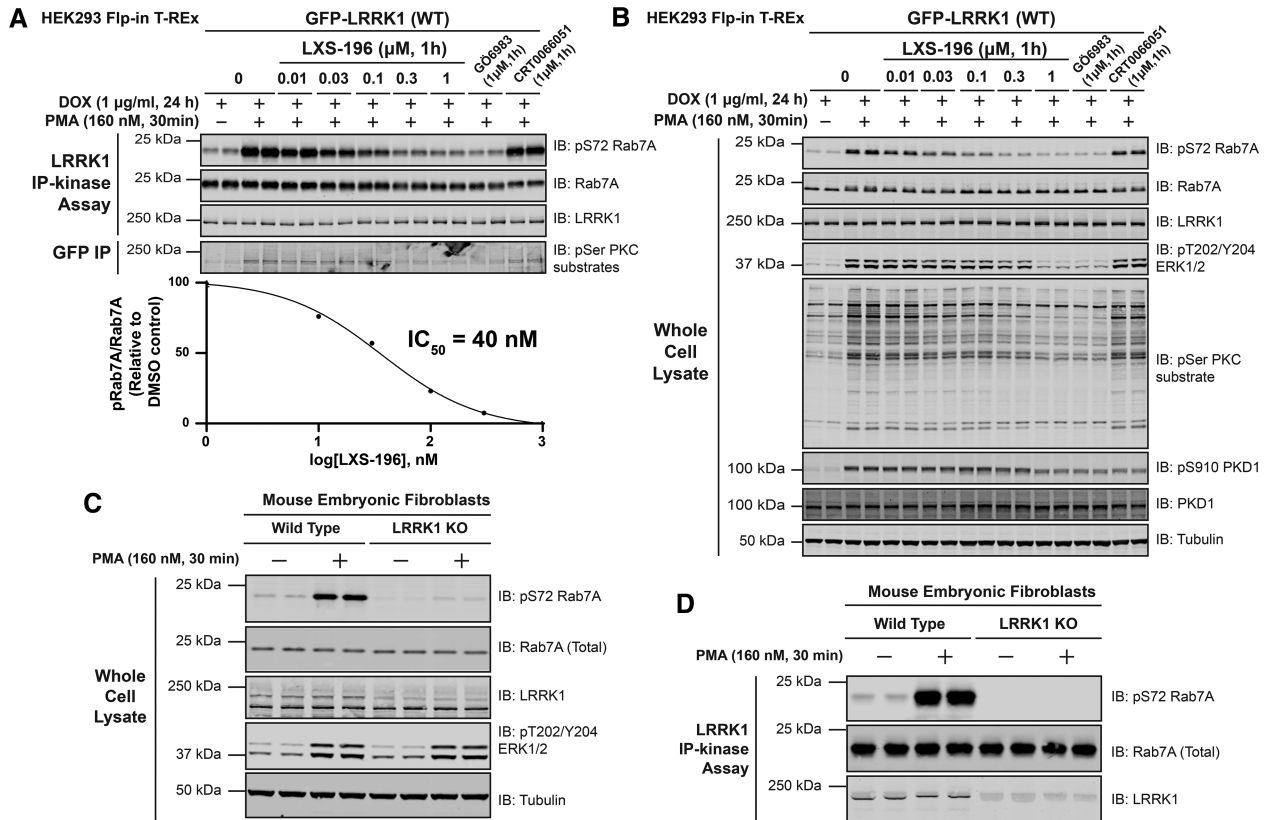


Figure 3. PMA induces phosphorylation and activation of immunoprecipitated LRRK1.

(A, upper panel) HEK293 Flp-In T-REx cells stably expressing wild type (WT) GFP-LRRK1 were treated with 1 $\mu\text{g/ml}$ doxycycline for 24 h to induce expression of GFP-LRRK1. Cells were then serum-starved for 16 h, incubated \pm the indicated concentration of LXS-196, GÖ6983 or CRT0066051. Thirty minutes prior to lysis, cells were stimulated \pm 160 nM phorbol 12-myristate 13-acetate (PMA) for 30 min and cell lysed. Upper panel- GFP-LRRK1 immunoprecipitated using an anti-GFP nanobody and LRRK1 kinase activity towards recombinant Rab7A assessed in a 30 min assay. Reactions were terminated by addition of SDS-sample buffer and levels of pSer72-Rab7A, Rab7A and LRRK1 were assessed by quantitative immunoblot analysis using the LI-COR Odyssey CLx Western Blot imaging system with the indicated antibodies. Combined immunoblotting data from two independent biological replicates (each performed in duplicate) are shown. (A, lower panel) Quantified immunoblotting data of LRRK1 kinase assays are presented as ratios of pRab7ASer72/total Rab7A (mean \pm SEM) vs concentration of LXS-196 relative to levels observed with no inhibitor added (100%). IC₅₀ values were calculated with GraphPad Prism (version 9.1.0) using non-linear regression analysis. Note that the blank value of basal LRRK1 activity observed in unstimulated cells with no inhibitor was subtracted from stimulated values for the IC₅₀ analysis (B) The whole cell extracts (10 μg) that were prepared in (A) were subjected to quantitative immunoblot analysis using the LI-COR Odyssey CLx Western Blot imaging system with the indicated antibodies. (C) As in (A) except wild type and homozygous LRRK1 knock-out primary Mouse Embryonic Fibroblasts (MEFs) were serum-starved for 16 h and stimulated \pm 160 nM PMA for 30 min and cells lysed. Whole cell extracts (10 μg) were prepared and subject to quantitative immunoblot analysis. (D) As in (C) except, endogenous LRRK1 was immunoprecipitated from whole cell extracts using a polyclonal total LRRK1 antibody and LRRK1 kinase activity towards recombinant Rab7A assessed in a 30 min assay. Phosphorylation off Rab7A was assessed by immunoblot analysis.

endogenous LRRK1 kinase activity and Rab7A phosphorylation in wild type but not in LRRK1 knockout cells (Figure 3C,D).

PKC isoforms phosphorylate and activate LRRK1-*in vitro*

We next tested whether recombinant PKC isoforms (PKC α , PKC β , PKC γ , PKC ϵ , PKC θ and PKC ζ) directly phosphorylated wild-type LRRK1[20-2015] and kinase inactive LRRK1[20-2015, D1409A]. Reactions were undertaken using a Mg- $[\gamma\text{-}^{32}\text{P}]\text{ATP}$ radioactive assay and phosphorylation monitored by autoradiography as well as by immunoblotting with the Pan phospho-PKC substrate antibody (Figure 4A). All PKC isoforms induced phosphorylation of wild type as well as kinase-inactive LRRK1[D1409A] to differing extents, with

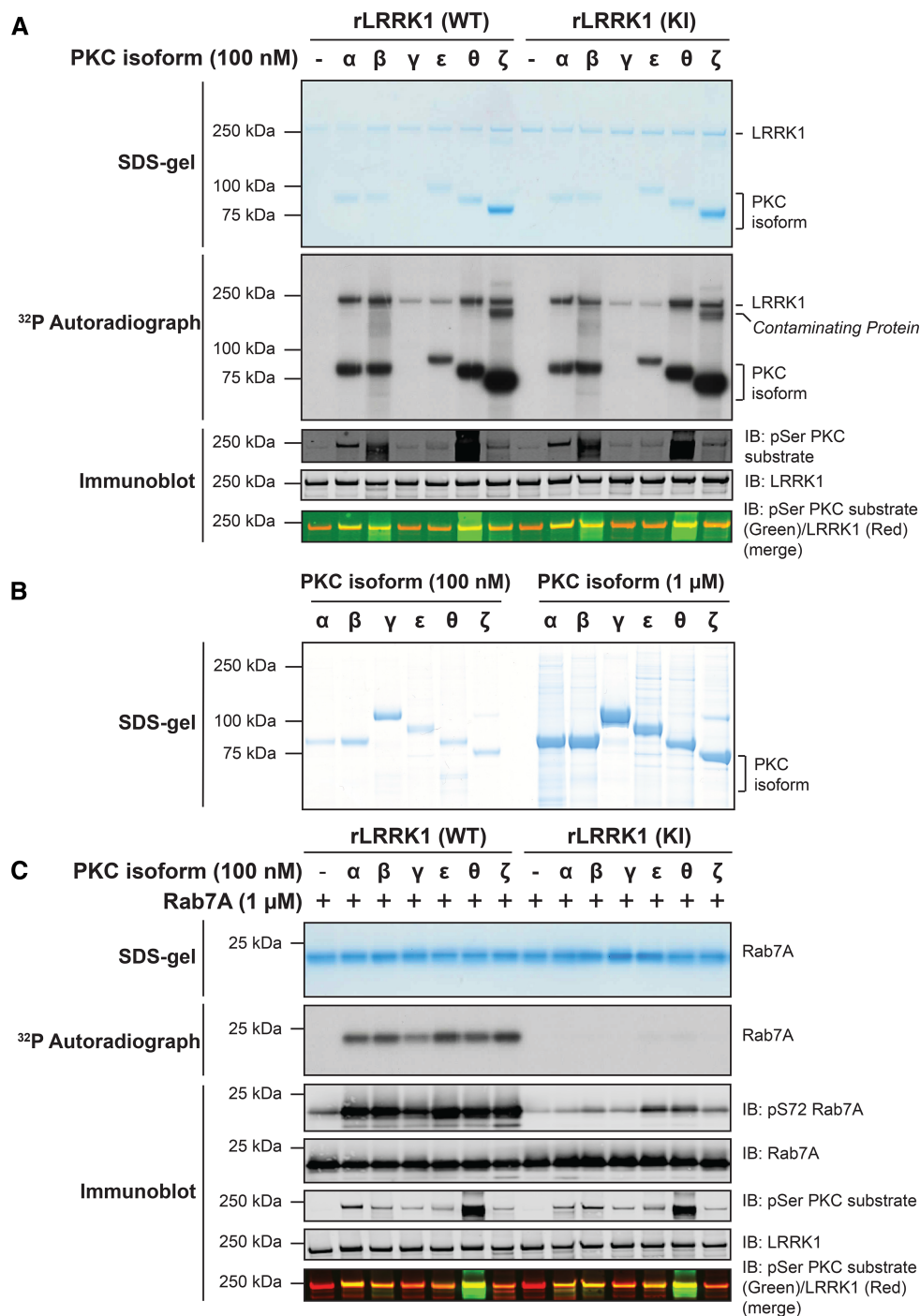


Figure 4. Recombinant PKC isoforms phosphorylate and activate LRRK1.

Part 1 of 2

(A) The indicated recombinant PKC isoforms (100 nM) were incubated with wild-type (WT) insect cell expressed recombinant (r) LRRK1[20-2015] or kinase inactive (KI) LRRK1[D1409A, 20-2015] (50 nM) in the presence of Mg[γ-³²P]ATP. Reactions were terminated after 30 min with SDS-sample buffer. 80% of each reaction was resolved by SDS-polyacrylamide electrophoresis, stained by Coomassie blue (upper panel), and subjected to autoradiography (middle panel). The remaining reaction mixture was subjected to a multiplexed immunoblot analysis using the LI-COR Odyssey CLx Western Blot imaging system to assess pan PKC substrate phosphorylation antibody (green channel) and total levels of LRRK1 protein (red channel) (lower panel). (B) Twenty microliters of 100 nM (left panel) or 1 μM (right panel), of the indicated PKC isoforms was used in panel (A) were subjected to polyacrylamide gel electrophoresis and stained with Coomassie blue. (C) The indicated recombinant PKC

Figure 4. Recombinant PKC isoforms phosphorylate and activate LRRK1.

Part 2 of 2

isoforms (100 nM) were incubated with recombinant wild-type LRRK1[20-2015] or kinase inactive LRRK1[D1409A, 20-2015] (50 nM) in the presence of non-radioactive MgATP for 30 min (Step-1 kinase assay). PKC phosphorylated LRRK1 was then diluted 1.5-fold into a kinase assay containing recombinant Rab7A (1 mM) in the presence of Mg[γ - 32 P]ATP (Step 2 of the kinase assay). Reactions were terminated after 30 min with SDS-sample buffer. Seventy-five percent of each reaction was subjected to SDS-polyacrylamide electrophoresis, stained by Coomassie blue (upper panel), and subjected to autoradiography (middle panel). The remaining reaction mixture was subjected to a multiplexed immunoblot analysis using the LI-COR Odyssey CLx Western Blot imaging system with the indicated antibodies (lower panel).

PKC α , PKC β , and PKC θ phosphorylating LRRK1 most strongly. Autophosphorylation of all PKC isoforms except for PKC γ was observed (Figure 4A). Although PKC γ was not detected in the reaction mixture it was observed in a Coomassie stained gel of the PKC isoforms panel used for this study (Figure 4B). It is possible that PKC γ became degraded during the kinase assay in this experiment. Additionally, in reactions employing PKC ζ , a protein band that is likely a phosphorylated contaminant in the PKC ζ preparation, is visible below the ~250 kDa LRRK1 band on the autoradiograph. Using Mg[γ - 32 P]ATP of known specific activity, we were able to estimate the stoichiometry of PKC α mediated phosphorylation of LRRK1. At the highest concentration of PKC α tested (100 nM), stoichiometry of phosphorylation was calculated to be 0.23 mol 32 P/mol protein (Supplementary Figure S2).

To determine whether PKC phosphorylation of LRRK1 stimulated kinase activity, we performed a two-step kinase assay. In the first step, recombinant wild-type LRRK1[20-2015] or kinase-inactive LRRK1[20-2015, D1409A], was incubated for 30 min with PKC isoforms (PKC α , PKC β , PKC γ , PKC ϵ , PKC θ and PKC ζ) in the presence of non-radioactive Mg-ATP. In the second step, an aliquot of this first reaction was assayed for its ability to phosphorylate Rab7A in the presence of Mg[γ - 32 P]ATP. Phosphorylation of Rab7A was monitored by 32 P-autoradiography as well as with a pSer72 Rab7A phospho-specific antibody. We observed that PKC phosphorylation of wild-type LRRK1[20-2015], but not kinase-inactive LRRK1[20-2015, D1409A], markedly boosted phosphorylation of Rab7A, with all PKC isoforms tested (Figure 4C). It should be noted that low levels of Rab7A phosphorylation at Ser72 was detected with PKC ϵ and PKC θ phosphorylation of kinase-inactive LRRK1[20-2015, D1409A] (Figure 4C), which is likely due to these PKC isoforms phosphorylating Rab7A to a very low stoichiometry, which can be detected using the high sensitivity phospho-specific antibody.

We next analyzed whether wild-type LRRK1 immunoprecipitated from unstimulated HEK293 cells could be activated by PKC α phosphorylation *in vitro*. For these studies we used PKC α as this is one of the most well studied isoforms and we were able to obtain sufficient enzyme and a high concentration for our analysis. We treated immunoprecipitated LRRK1 with increasing doses of recombinant PKC α (10 to 300 nM) for 30 min in the presence of Mg $^{2+}$ ATP and subsequently measured phosphorylation of Rab7A employing a phospho-specific antibody (Figure 5A). Increased Rab7A phosphorylation was detected in this assay using 30 nM PKC α , plateauing at an enzyme concentration of 100 nM. Similar results were obtained from an equivalent experiment in which recombinant LRRK1[20-2015] produced in insect cells was phosphorylated with increasing amounts of PKC α (Supplementary Figure S3A). We next performed a time course of activation of LRRK1 using 100 nM PKC α and found that LRRK1 activation was detected after 5 min incubation and plateaued at 40 min (Figure 5B). Similar results were obtained in an analogous experiment employing insect cell-produced recombinant LRRK1[20-2015] (Supplementary Figure S3B). We also found that the activity of phorbol ester-stimulated LRRK1 was moderately enhanced by PKC α phosphorylation *in vitro* (Supplementary Figure S4).

Consistent with phosphorylation triggering activation of LRRK1, incubation of immunoprecipitated activated LRRK1 derived from phorbol ester stimulated cells, with lambda phosphatase, reduced LRRK1 activity to levels observed in unstimulated cells (Figure 5C). This effect was largely prevented by using lambda phosphatase that had been preincubated with EDTA to suppress phosphatase activity (lambda phosphatase is a magnesium dependent phosphatase [42]) (Figure 5C).

PKC α phosphorylates LRRK1 at three conserved residues lying in the GTPase COR $_B$ domain

Kinase inactive LRRK1[20-2015, D1409A] was next phosphorylated *in vitro* in the presence or absence of PKC α , subjected to SDS-polyacrylamide gel electrophoresis, and digested with Trypsin + Lys-C (Figure 6A).

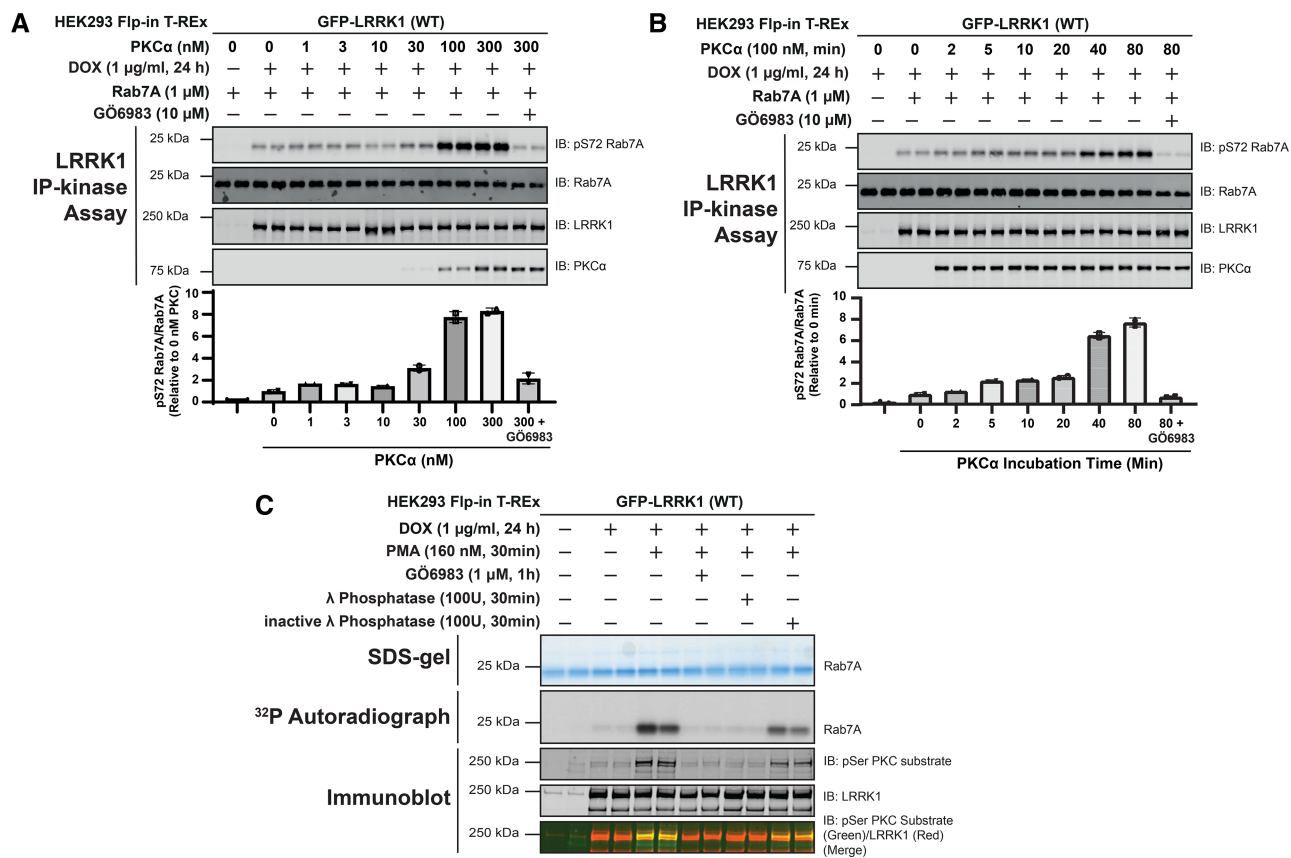


Figure 5. Time-course, dose-dependence, and reversibility of activation of LRRK1 by PKCα.

(A) HEK293 Flp-in T-REx cells stably expressing wild type (WT) GFP-LRRK1 were treated ± 1 µg/ml doxycycline for 24 h to induce GFP-LRRK1 expression. Cells were serum-starved for 16 h, lysed and GFP-LRRK1 immunoprecipitated and aliquoted as indicated. Each aliquot contains GFP-LRRK1 immunoprecipitated from 1 mg of HEK293 cell lysate. Step-1 of the LRRK1 kinase activation assay was setup by incubating GFP-LRRK1 aliquots with the indicated concentrations of PKCα and ±inhibitor GÖ6983 (10 µM) in the presence of non-radioactive MgATP for 30 min. PKC phosphorylated LRRK1 was then diluted 1.5-fold into a kinase assay containing recombinant Rab7A (1 µM) in the presence of non-radioactive MgATP (Step 2 of the kinase assay). Reactions were terminated after 30 min with SDS-sample buffer analysed by multiplexed immunoblot analysis using the LI-COR Odyssey CLx Western Blot imaging system with the indicated antibodies (upper panel). Combined immunoblotting data from two independent biological replicates (each performed in duplicate) are shown. Lower panel quantified immunoblotting data are presented as ratios of pRab7ASer72/total Rab7A (mean ± SEM) relative to levels observed with no PKCα added (given a value of 1.0).

(B) As in (A) except in step 1 of the kinase activity assay 100 nM PKCα was incubated with immunoprecipitated GFP-LRRK1 for the times indicated.

(C) As in (A) except that following serum starvation, cells were treated stimulated ± 160 nM phorbol 12-myristate 13-acetate (PMA) for 30 min and cells lysed. GFP-LRRK1 was immunoprecipitated from 1 mg of cell lysate incubated ± 100U of either active or 10 mM EDTA-inactivated λ phosphatase for 30 min. Following the phosphatase treatment, the beads were extensively washed and LRRK1 was subjected to kinase assay with recombinant Rab7A using Mg[γ-³²P]ATP. Seventy-five percent of each reaction was subjected to SDS-polyacrylamide electrophoresis, stained by Coomassie blue (upper panel), and subjected to autoradiography (middle panel). The remaining reaction mixture was subjected to a multiplexed immunoblot analysis using the LI-COR Odyssey CLx Western Blot imaging system with the indicated antibodies (lower panels). Combined immunoblotting data from two independent biological replicates (each performed in duplicate) are shown.

The resultant peptides were analyzed either by Electron Activated Dissociation (EAD) on a ZenoTOF 7600 mass spectrometer or Higher energy Collisional Dissociation (HCD) on an orbitrap instrument, without phospho-peptide enrichment (Figure 6B and Supplementary Figure S5). These analyses revealed a cluster of four phosphorylation sites regulated by PKCα phosphorylation, located within a loop of the COR_B domain (Thr1061, Ser1064, Ser1074 and Thr1075) (Figure 6B). The Thr1061 site was identified using both EAD and HCD fragmentation, Ser1064 was detected by the HCD method and the dual phosphorylated peptide encompassing Ser1074 and Thr1075 was detected using EAD method (Figure 6B and Supplementary Figure S4).

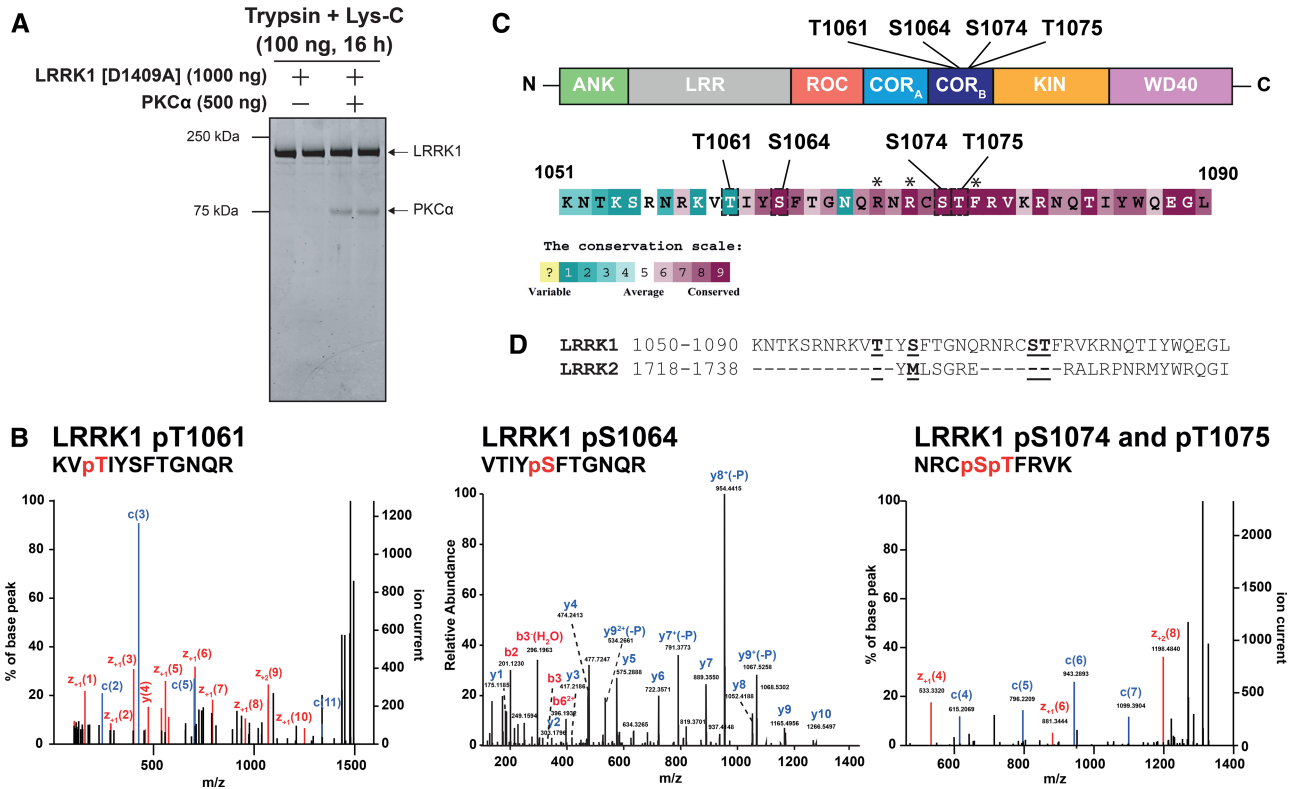


Figure 6. Identification of Ser1064, Ser1074 and Thr1075 as the key PKC-regulated sites on LRRK1.

(A) Kinase inactive LRRK1[D1409A, 20–2015] (200 nM) was incubated ± PKCα (400 nM) in the presence of MgATP. Reactions were terminated after 30 min with SDS-sample buffer and reactions resolved by SDS-polyacrylamide electrophoresis and gel stained by Coomassie blue. (B) The gel bands containing LRRK1 were digested with mixture of trypsin and Lys-C and the resultant peptides analyzed by Electron Activated Dissociation on a ZenoTOF 7600 mass spectrometer without phospho-peptide enrichment. The annotated MS/MS spectra of the three key PKC phosphorylated phosphosites encompassing phosphorylated Thr1061, phosphorylated Ser1064 and doubly phosphorylated Ser1074 and Thr1075 are shown. These sites were only detected in the LRRK1 samples phosphorylated with PKCα. Annotated MS/MS spectra of key PKC regulated phosphosites. MS/MS spectra of pT1061 and pS1064 were identified from HCD fragmentation acquired on Orbitrap Exploris 240 MS platform and the coverage of b and y ion series are denoted by red and blue color text, respectively. MS/MS spectrum of a dual phosphorylated peptide of pS1074 and pT1075 sites were identified from EAD fragmentation acquired on Sciex Zeno-TOF 7600 platform. The EAD fragmentation enables accurate site localization and the coverage for c and z ion series were denoted with blue and red color text. (C) Upper panel displays the location within the COR_B domain arrangement of the Thr1061, Ser1064, Ser1074 and Thr1075 PKCα phosphorylation sites on the domain structure of LRRK1. Lower panels show the amino acid sequences encompassing the PKCα phosphorylation sites and their evolutionary conservation score from 1 (least conserved) to 9 (most conserved) of each residue determined calculated the Consurf server (<https://consurf.tau.ac.il/>) [53]. Sequences of LRRK1 homologs were obtained from OrthoDB (<https://www.orthodb.org/>) [54] and alignment of sequences was performed using the MAFFT server (<https://www.ebi.ac.uk/Tools/msa/mafft/>) [55]. Subsequently, alignment is inserted into the Consurf server, with the sequence for human LRRK1 indicated as the query sequence (Taxonomy code 9606) and conservation scores are determined. Lower panel displays the conservation score scales utilized by the Consurf server. Residues lying at the −5, −3 and +1 position of the Thr1075 phosphorylation site that confer optimal specificity for PKC isoform phosphorylation and marked with an asterisks (D) Sequence alignment of LRRK1 and LRRK2 surrounding the LRRK1 PKC phosphorylation sites showing that amino acid sequence across this region is not conserved between LRRK1 and LRRK2.

Conservation evolutionary analysis employing the Consurf motif platform demonstrated that Ser1064 (score 9), Ser1074 (score 9) and Thr1075 (score 9) are highly conserved, but Thr1061 (score 1) is not. Significantly, Thr1075 lies within the optimal PKC consensus phosphorylation motif comprising basic Arg residues at the −3 and −5 positions in addition to a hydrophobic Phe residue at the +1 position [29] and these residues also display the highest conservation score of 9 (Figure 6C). Interestingly, these residues are located within a motif that is not conserved in LRRK2 (Figure 6D). We also used the HCD method to analyze phosphosites on LRRK1[20–2015, D1409A] ± phosphorylation with PKCα employing two additional protease digests (Asp-N

and chymotrypsin) (Supplementary Figure S5). This led to the identification of additional sites, several not induced by PKC α phosphorylation, that are likely phosphorylated by other kinases in insect cells. Previous work by the Taymans and Greggio laboratories had previously reported the Ser1075 and Thr1075 sites as well as three other sites we did not detect in our analysis (Ser249, Ser1241 and Thr1287) from SH-SY5Y neuroblastoma cell lines stably expressing 3xFlag-LRRK1 [43].

PKC activation of LRRK1 is mediated by phosphorylation of Ser1064, Ser1074 and Thr1075

To explore the importance of the cluster of Thr1061, Ser1064, Ser1074 and Thr1075 PKC phosphorylation sites, we mutated these individually or in combination to Ala, to block phosphorylation (Figure 7A) or to Glu to mimic phosphorylation (Figure 7B). We found that mutation of Thr1075 to Ala alone, essentially blocked LRRK1 activation, whereas individual mutation of the other Ser1064 or Ser1074 only modestly impacted activity. Mutation of Thr1061 that has a low evolutionary conservation score suggesting that it would not play a critical role, had no effect (Figure 7A). The basal activity of the individual Ser1064Ala, Ser1074Ala and Thr1075Ala mutants were similar or marginally lower than that of wild-type LRRK1 and significantly higher than that observed with kinase inactive LRRK1 (Figure 7A). Combined mutation of Ser1064Ala, Ser1074Ala and Thr1075Ala, reduced LRRK1 basal activity significantly and ablated phorbol ester induced activation (Figure 7A).

A triple Ser1064Glu, Ser1074Glu and Thr1075Glu mutant, displayed ~3-fold increased basal activity and was not activated further by phorbol ester treatment (Figure 7B). Individual mutation of Ser1064 to Glu had no impact on the basal or phorbol ester induced activation of LRRK1, though mutating Ser1074 to Glu induces almost doubled kinase activity compared with the wild-type protein following phorbol ester treatment (Figure 7B). We found that Thr1075 to Glu inhibited LRRK1 activity and blocked its activation by phorbol ester.

LRRK1 co-localizes with PKC α at the plasma membrane following phorbol ester stimulation

To investigate the localization of LRRK1, PKC α and Rab7A, we performed subcellular fractionation, generating membrane and cytosol fractions from unstimulated and phorbol ester stimulated cells. This revealed that as expected PKC α was mainly in the cytosol fraction in unstimulated cells and translocated to the membrane following phorbol ester stimulation (Figure 8A). LRRK1 was located both in the cytosol and membrane fractions and its distribution was not impacted by phorbol ester treatment. Most Rab7A and essentially all pSer72Rab7A were only observed in the membrane fraction (Figure 8A). The cytosolic fraction of total Rab7A is likely to represent the portion of the protein that is bound to GDI in cytosol. Immunofluorescence studies employing rapid immersion of cover slips in liquid nitrogen to extrude cytosolic proteins and enrich for membrane-associated proteins, confirmed that a significant proportion of LRRK1 was localized at the plasma membrane and that phorbol ester induced recruitment of PKC α to the plasma membrane, resulting in co-localization with the plasma membrane marker Na-K ATPase (Figure 8B and Supplementary Figure S6). We observed a robust increase in pSer72 Rab7A staining with phorbol ester stimulation, though no obvious co-localization with LRRK1 is observed (Figure 8C). This study indicates that the pRab7A monoclonal antibody is suitable for immunofluorescence studies. We also observed that mutation of Ser1064, Ser1074 and Thr1075 to either Ala or Glu did not markedly influence the localization of LRRK1 observed (Supplementary Figure S7).

Discussion

Our key finding is that PKC isoforms directly activate LRRK1 by phosphorylating a cluster of three highly conserved PKC phosphorylation sites located on a loop of the COR_B domain (Ser1064, Ser1074 and Thr1075). Our data are consistent with a model in which phosphorylation of Thr1075, that lies within an optimal PKC phosphorylation motif, promotes phosphorylation of Ser1064 and Thr1074 that do not lie within optimal PKC site motifs, and that all three phosphorylation sites contribute to activity. Our data suggest that the Thr1075Glu mutation alone without phosphorylation of the two nearby residues results in loss of LRRK1 activity. It is possible that the Glu mutation is unable to mimic phosphorylation and induces a conformational change that is detrimental to basal kinase activity. It is also possible that phosphorylation of Thr1075 without concomitant phosphorylation of Ser1064 and Ser1074 is insufficient to activate LRRK1. Interestingly mutation of the adjacent Ser1074 site to Glu did not impact basal activity significantly, but enhanced phorbol ester stimulated activity 2-fold above that of the wild type. Thus, the most active species of LRRK1 that we have tested

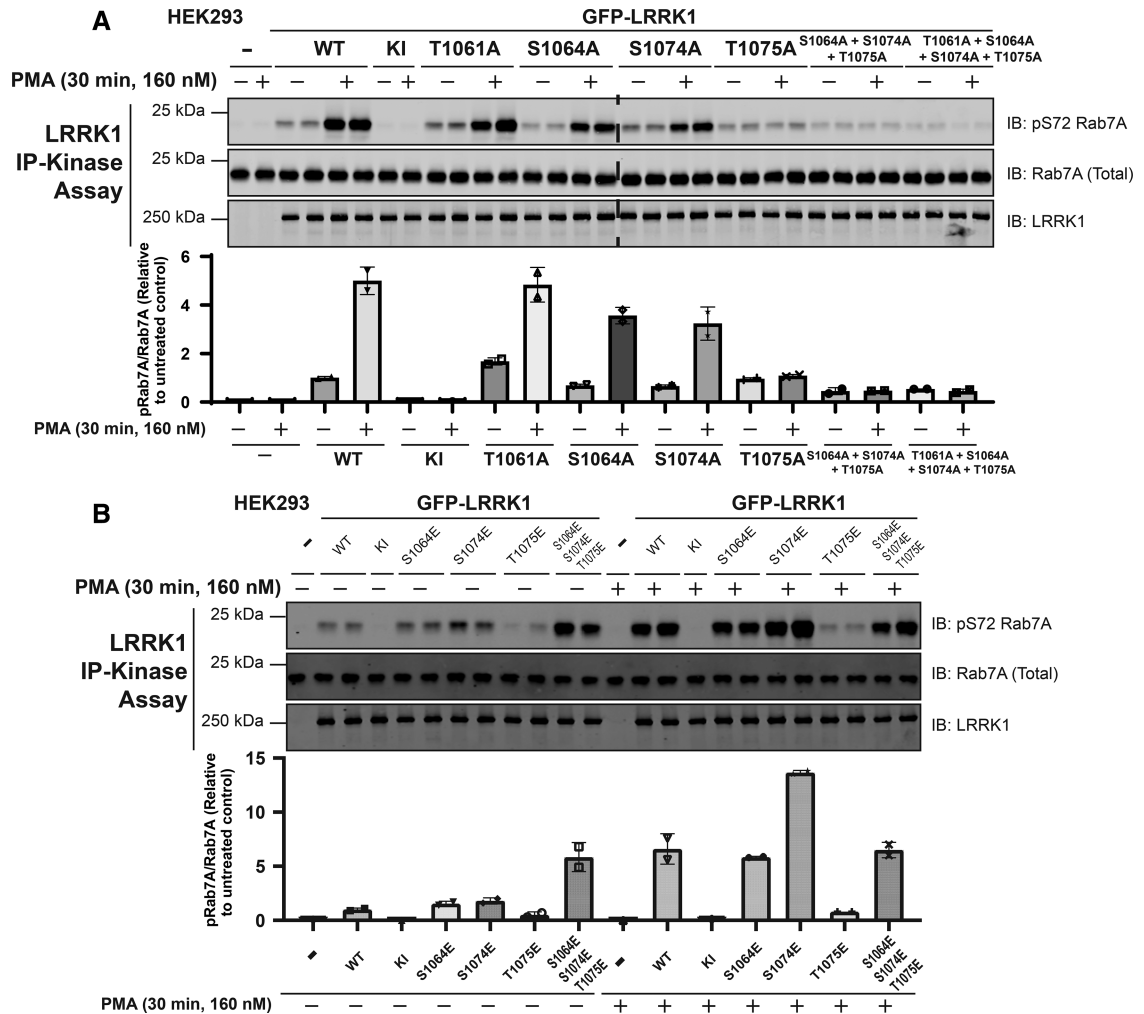


Figure 7. Mutations to Ser1064, Ser1074 and Thr1075 impact phorbol ester dependent LRRK1 activation.

(A and B) HEK293 cells were transiently transfected with plasmids encoding wild type (WT), kinase-inactive (KI) LRRK1 [D1409A] or the indicated mutants of GFP-LRRK1. Ala mutants to block phosphorylation were studied in (A) and Glu mutants to mimic phosphorylation were investigated in (B). Twenty-four hours post transfection, cells were serum-starved for 16 h and stimulated ± 160 nM phorbol 12-myristate 13-acetate (PMA) for 30 min. Cells were lysed and GFP-LRRK1 immunoprecipitated using an anti-GFP nanobody from 1 mg of cell extract. LRRK1 kinase activity towards recombinant Rab7A was assessed in a 30 min assay. Reactions were terminated by addition of SDS-sample buffer and levels of pSer72-Rab7A, Rab7A and LRRK1 were assessed by quantitative immunoblot analysis using the LI-COR Odyssey CLx Western Blot imaging system with the indicated antibodies. Combined immunoblotting data from two independent biological replicates (each performed in duplicate) are shown. Lower panel quantified immunoblotting data are presented as ratios of pRab7ASer72/total Rab7A (mean ± SEM) relative to levels observed with the activity of non-stimulated wild-type LRRK1.

is the LRRK1[S1074E] mutant stimulated with phorbol ester (Figure 7B). In our mass spectrometry studies, we only observed a doubly phosphorylated Ser1074 and Thr1075 peptide, which also suggests that both these sites are efficiently phosphorylated by PKC isoforms. In future work it would be interesting to explore how phosphorylation of Thr1075 might regulate phosphorylation of the Ser1064 and Ser1074 residues. The Ser1064 and Ser1074 residues are unlikely to represent autophosphorylation sites, as the PKC phosphorylation site peptide mapping studies we undertook were performed using kinase-inactive LRRK1[20-2015, D1409A]. We and others [43], have also identified several additional phospho-sites on LRRK1, some of which have a high evolutionary score and likely to be phosphorylated in insect cells (Supplementary Figure S5); further work is required to study any roles that these sites might play. The Ser1064, Ser1074 and Thr1075 or the residues

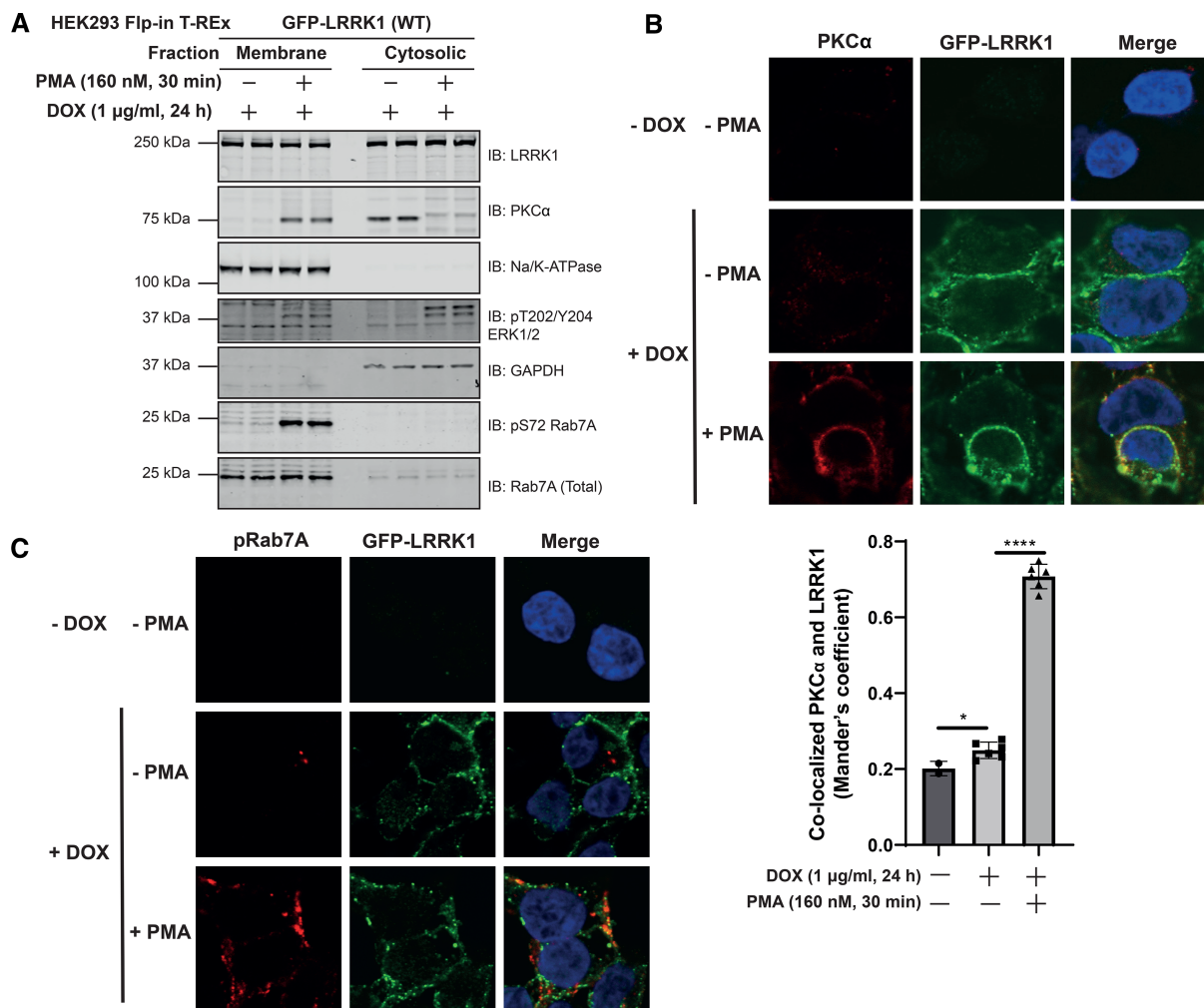


Figure 8. Phorbol ester induces co-localization of PKC α and LRRK1 at the plasma membrane.

HEK293 Flp-In T-REx cells stably expressing wild type (WT) GFP-LRRK1 were treated with 1 μ g/ml doxycycline for 24 h to induce GFP-LRRK1 expression. Cells were serum-starved for 16 h, and stimulated \pm 160 nM phorbol 12-myristate 13-acetate (PMA) for 30 min. Next, cells were resuspended in a hypotonic solution (500 μ l) and homogenized by passing through a 25-G needle. Extracts were fractionated into membrane and cytosolic fractions through high-speed ultracentrifugation. Membrane fractions were resuspended to the same volume as extract used for ultracentrifugation and equal volumes (500 μ l) were assessed by quantitative immunoblot analysis using the LI-COR Odyssey CLx Western Blot imaging system with the indicated antibodies. Combined immunoblotting data from two independent biological replicates (each performed in duplicate) are shown. (B, top panel) As in (A) except cells were grown on coverslips and following treatments they were permeabilized by liquid nitrogen freeze-thaw to deplete cytosol [49] and then fixed and stained with mouse anti-PKC α , chicken anti-GFP and DAPI. (B, bottom panel) Co-localization of GFP-LRRK1 and PKC α was determined from a Mander's coefficient (presented as mean \pm SEM) after automatic thresholding. * P < 0.05, **** P < 0.0001 by Student's unpaired, two-tailed t -test. (C) As in (B, upper panel) except cells are stained with rabbit anti-pS72 Rab7A and chicken anti-GFP.

encompassing these are not conserved in LRRK2 (Figure 6D) which likely accounts for why LRRK2 is not activated by PKC phosphorylation.

Recent work has reported a 5.8 Å Cryo-EM structure of the monomeric ROC-COR-Kinase-WD40 (RCKW) fragment of LRRK1 in the inactive conformation [2]. Although COR_B localized close to the kinase domain, it was not possible to model how PKC phosphorylation of the COR_B would impact the structure of LRRK1. The α C-helix is a universally conserved helix which is positioned centrally, between the N and C lobes of the kinase domain. The orientation of the helix is critical in kinase regulation with the distance between the N-terminal of the α C-helix and the activation loop defining the open and closed confirmations [44]. The AlphaFold [45]

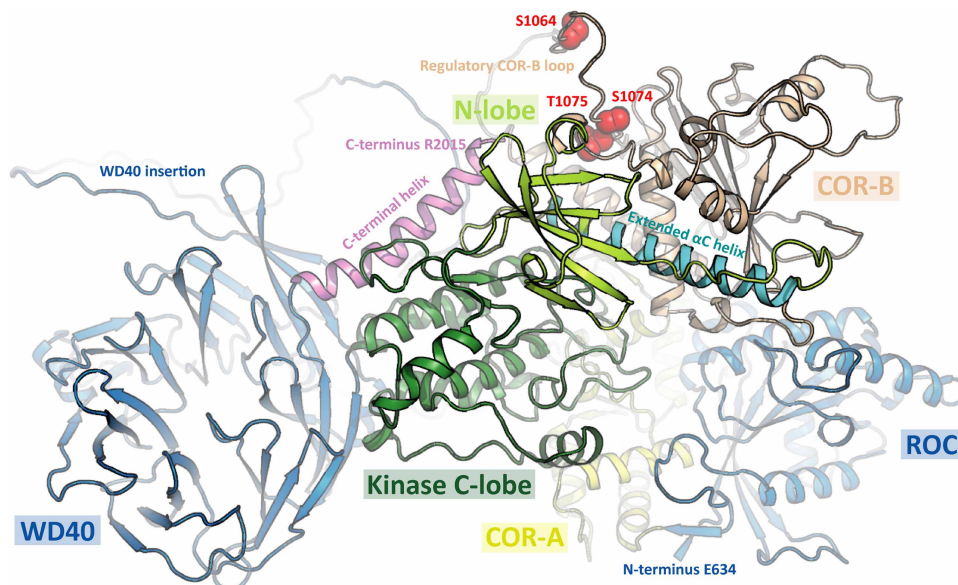


Figure 9. Model of LRRK1 structure.

Prediction of LRRK1 (Q38SD2) structure as determined by AlphaFold Protein Structure Database (<https://alphafold.ebi.ac.uk/entry/Q38SD2>). Location of phosphosites (Ser1064, Ser1074 and Thr1075) within a disordered region are highlighted in red. The N-terminal ANK and LRR domains were omitted for clarity.

predicted structure of LRRK1 (<https://alphafold.ebi.ac.uk/entry/Q38SD2>), appears to be in the active conformation with a well ordered α C-helix. However, the region containing the Ser1064, Ser1074 and Thr1075 PKC phosphorylation sites is disordered which makes it difficult to predict how phosphorylation the COR_B loop impacts folding and interaction with the kinase α C-helix (Figure 9). We speculate that phosphorylation of LRRK1 promotes ordering of residues in this region triggering stabilization of the α C-helix through an unknown mechanism. The current version of AlphaFold does not predict how phosphorylation impacts the structure. Recently, a 3.5 Å structure of an active tetrameric form of LRRK2 has been reported [18]. This consists of two peripheral LRRK2 molecules in the inactive conformation and two central LRRK2 protomers in an active conformation [18]. The residues in LRRK2 that lie at the equivalent region to Ser1064, Ser1074 and Thr1075 in the active LRRK2 subunits encompass residues 1721–1725 in LRRK2 (Figure 9, Figure 6C). Interestingly, in the active LRRK2 conformation, the 1721–1725 residues point towards the kinase domain and interact directly with the kinase α C-helix [18]. Furthermore, in a recent hydrogen-deuterium exchange mass spectrometry (HDX-MS) study, when the Type I inhibitor MLI-2 was added to induce the active conformation of LRRK2, stabilization of these 1721–1725 COR_B residues was observed [46]. The prediction from these observations was that phosphorylation of Ser1064, Ser1074 and Thr1075 could activate LRRK1 by engaging crosstalk between the C-terminal/ α C-helix and Dk-helix, which is observed in the active state of LRRK2 (Figure 9). It would also be interesting to compare the subunit structures of the inactive and PKC phosphorylated active LRRK1. The finding that LRRK1 activity was inhibited by Triton-X100 could be explained if this disrupted multimeric subunit assembly required for activation (Figure 2A).

Based on our *in vitro* analysis all conventional and novel PKC isoforms that were tested activated LRRK1 to a similar level, suggesting that LRRK1 has evolved to be activated by multiple PKC isoforms. We observed that relatively low stoichiometry of PKC phosphorylation of ~ 0.23 mol ^{32}P /mol protein was sufficient to activate LRRK1 ~ 100 -fold (Figure 4B and Supplementary Figure S2). Allowing for three PKC phosphorylation sites, theoretical maximal stoichiometry of phosphorylation of LRRK1 would be three. Therefore, PKC phosphorylation can be estimated to enhance LRRK1 activity ~ 1000 -fold emphasizing the major effect that phosphorylation has. The reasons for the relatively low phosphorylation levels of recombinant LRRK1 observed could be due the lack of enzyme and/or factors such as scaffolding proteins and/or membranes not being present in our *in vitro* reaction. After PKD, LRRK1 is to our knowledge the second protein kinase to be directly activated by PKC isoforms. It would be interesting to explore whether any previously described biology controlled by PKC

isoforms is mediated through activation of LRRK1 and development of specific LRRK1 inhibitors would help address this question. It is also possible that other protein kinases including AGC kinases that are related to PKC isoforms and display similar substrate specificity, could also activate LRRK1 by phosphorylating Ser1064, Ser1074 and Thr1075. Further work would be required to study this and pinpoint which PKC isoform(s) mediate LRRK1 activation *in vivo*. It would also be important to generate phosphospecific antibodies that detect Ser1064, Ser1074 and Thr1075 phosphorylated activated form LRRK1 to better probe the function of the active form of this enzyme,

Materials and methods

Reagents

[γ -³²P]ATP was purchased from PerkinElmer. Phorbol 12-myristate 13-acetate (PMA) (#P8139), was purchased from Sigma–Aldrich. PKC-specific inhibitors GÖ6983 (#S2911), CRT0066051 (#S3422) and LXS-196 (#S6723) were purchased from Selleckchem. CHAPS hydrate (#C5070) and Digitonin (#D141) were purchased from Sigma–Aldrich. L- α -Phosphatidylserine (#840032C) and L- α -Diacylglycerol (#800815C) were purchased from Avanti Polar Lipids, Inc. Lambda Protein Phosphatase (#P0753S) was purchased from New England Biolabs. Trypsin/Lys-C mix (#V5073), Chymotrypsin (#V1062) and Asp-N (#V1621) were purchased from Promega. Bryostatin-1 (#2383) was purchased from TOCRIS. Recombinant Rab7A protein was expressed and purified as previously described [8]. Recombinant insect cell expressed PKC isoforms namely His-PKC α (DU5084), His-PKC β (DU33630), Glutathione-S-transferase -PKC γ (DU30188) His-PKC ϵ (DU33642), His-PKC θ (DU29920) and PKC ζ (DU1447) were obtained from MRC Reagents and Services (<https://mrcintranet.lifesci.dundee.ac.uk>).

Plasmids

All plasmids used in this study were obtained from the MRC PPU Reagents and Services (<https://mrcpureagents.dundee.ac.uk>). Each plasmid was confirmed by sequencing at the MRC Sequencing and Services (<https://www.dnaseq.co.uk>) and are available to request via the MRC PPU Reagents and Services website (<https://mrcpureagents.dundee.ac.uk>).

Table 2 List of all plasmids used in this study

DU number	Construct	Vector
DU30382	GFP-LRRK1 wt	pcDNA5 FRT/TO
DU67084	GFP-LRRK1 [D1409A]	pcDNA5 FRT/TO
DU72350	GFP-LRRK1 [T1061A]	pcDNA5 FRT/TO
DU68548	GFP-LRRK1 [S1064A]	pcDNA5 FRT/TO
DU72349	GFP-LRRK1 [S1074A]	pcDNA5 FRT/TO
DU72411	GFP-LRRK1 [T1075A]	pcDNA5 FRT/TO
DU72383	GFP-LRRK1 [S0164A + S1074A + T1075A]	pcDNA5 FRT/TO
DU72351	GFP-LRRK1 [T1061A + S0164A + S1074A + T1075A]	pcDNA5 FRT/TO
DU68549	GFP-LRRK1[S1064E]	pcDNA5 FRT/TO
DU72553	GFP-LRRK1[S1074E]	pcDNA5 FRT/TO
DU72554	GFP-LRRK1[T1075E]	pcDNA5 FRT/TO
DU72619	GFP-LRRK1[S0164E + S1074E + T1075E]	pcDNA5 FRT/TO
DU13162	pOG44 Flp-Recombinase Expression Vector	pcDNA5
DU5084	His-PKC α	pFB HTB
DU33630	His-PKC β	pFB HTB
DU30188	Glutathione-S-transferase-PKC γ	BAC
DU33642	His-PKC ϵ	pFB HTB
DU29920	His-PKC θ	pFB HTB
DU1447	His-PKC ζ	pFB HTB

Table 3 List of all antibodies used in this study

Antibody target	Company	Catalogue No.	Host Species	Dilution
LRRK1 (1695-end)	MRC Reagents and Services	DU13868	Sheep	1 µg/ml
pSer72 Rab7A	Abcam Inc.	ab302494	Rabbit	1 : 1000
pThr73 Rab10	Abcam Inc.	ab230261 RRID: AB_2811274	Rabbit	1 : 1000
PKCα	Abcam Inc.	ab32376 RRID: AB_777294	Rabbit	1 : 1000
Na-K ATPase	Abcam Inc.	ab76020 RRID: AB_1310695	Mouse	1 : 10 000
Total Rab7A	Sigma	R8779 RRID: AB_609910	Mouse	1 : 2000
Total Rab10	Nanotools	0680-100/Rab10-605B11 RRID: AB_2921226	Mouse	1 : 500
LRRK2 (C-terminus)	NeuroMab	75-253 RRID: AB_10675136	Mouse	1 : 1000
α-Tubulin	Cell Signaling Technologies	3873S RRID: AB_1904178	Mouse	1 : 10 000
pThr202/Tyr204 ERK1/2	Cell Signaling Technologies	9101 RRID: AB_331646	Rabbit	1 : 1000
Total ERK1/2	Cell Signaling Technologies	9102 RRID: AB_330744	Rabbit	1 : 1000
p-Ser PKC Substrate	Cell Signaling Technologies	2261 RRID: AB_330310	Rabbit	1 : 1000
pSer916 PKD1	Cell Signaling Technologies	2051 RRID: AB_330841	Rabbit	1 : 1000
Total PKD1	Cell Signaling Technologies	90039 RRID: AB_2800149	Rabbit	1 : 1000
GAPDH	Santa Cruz Biotechnology	sc-32233 RRID: AB_627679	Mouse	1 : 5000

Antibodies

All antibodies were diluted in 5% (w/v) BSA (bovine serum albumin) in TBST Buffer (20 mM Tris-HCl pH 7.5, 0.15 M NaCl and 0.1% (v/v) Tween-20) and used for immunoblotting analysis at the indicated concentration or dilution. The phospho-specific Rab10 antibodies have been described previously [47].

LRRK1 KO primary MEF generation

Wild-type and homozygous LRRK1 knock-out MEFs were isolated from littermate-matched mouse embryos at day E12.5 resulting from crosses between heterozygous wild-type/KO mice as described previously [8].

Cell culture and lysis

HEK293 wild type (ATCC, #CRL-1573) and HEK293 Flp-in T-REx (ThermoFisher, #R78007) wild-type cells were cultured in Dulbecco's Modified Eagle's Medium (DMEM; GIBCO, #11960-085) containing 10% (v/v) fetal bovine serum (Sigma, #F7524), 2 mM L-glutamine (GIBCO, #25030024), 100 U/ml penicillin-streptomycin (Invivogen, #15140122). HEK293 Flp-in T-REx wild-type cells were grown in DMEM containing 10% (v/v) fetal bovine serum, 2 mM L-glutamine, 100 U/ml penicillin-streptomycin supplemented with 15 µg/ml Blastidicin (Invivogen, #ant-bl-10p) and 50 µg/ml Zeocin (Invivogen, #ant-zn-5). MEFs were grown in DMEM containing 10% (v/v) fetal bovine serum, 2 mM L-glutamine, 100 U/ml penicillin-streptomycin, supplemented with 1 mM sodium pyruvate (GIBCO, #11360-039) and non-essential amino acids (GIBCO, #11140-035). All

cells were incubated at 37°C, 5% CO₂ (v/v) in a humidified atmosphere and regularly tested for mycoplasma contamination. Cells were lysed in an ice-cold lysis buffer containing 50 mM HEPES, pH 7.4, 0.3% CHAPS hydrate (v/v), 270 mM sucrose, 150 mM NaCl, 1 mM sodium orthovanadate, 50 mM NaF, 10 mM 2- glycerophosphate, 5 mM sodium pyrophosphate, 1 µg/ml microcystin-LR (Enzo Life Sciences, #ALX-350-012-M001) and complete EDTA-free protease inhibitor cocktail (Sigma, #11836170001). Lysates were clarified by centrifugation at 20 800g at 4°C for 10 min and supernatant protein concentrations quantified using the Bradford assay kit (ThermoFisher, #23236).

Generation of HEK293 Flp-in T-REx stable cell lines

Non-transfected HEK293 Flp-in T-REx wild-type cells were seeded into 10 cm dishes at 4.5×10^6 cells/well. Cells were transfected using Polyethylenimine method [48]. Briefly, 0.5 µg of LRRK1 or LRRK2 plasmids, 4.5 µg of pOG44 Flp-Recombinase Expression Vector (ThermoFisher, #V600520) and 15 µl of 1 mg/ml PEI were added to 1 ml OptiMEM reduced serum media (GIBCO, #31985-062) and vortexed for 20 sec. Solution was then incubated at room temperature for 20 min to allow the formation of DNA-PEI complexes. Transfection mixes were subsequently added to cell culture medium and allowed to incubate at 37°C. Twenty-four hours post transfection, cells were selected for successful transfection using DMEM containing 10% (v/v) fetal bovine serum, 2 mM L-glutamine, 100 U/ml penicillin, and 100 µg/ml streptomycin supplemented with 15 µg/ml Blasticidin and 100 µg/ml Hygromycin (Invivogen, #ant-hg-5) for 48 h. Cells were then allowed to recover from selection in Hygromycin by incubation in DMEM containing 10% (v/v) fetal bovine serum, 2 mM L-glutamine, 100 U/ml penicillin-streptomycin for 1 week.

Transient and stable overexpression experiments and cell treatments

Twenty-four hours prior to transfection or treatment, HEK293 cells were seeded into 10 cm dishes at 4.5×10^6 cells/well. Cells were transfected using Polyethylenimine method [48], as described above. Briefly, 5 µg of LRRK1 plasmids and 15 µl of 1 mg/ml PEI were added to 1 ml OptiMEM reduced serum media (GIBCO, #31985-062) and vortexed for 20 sec. Solution was then incubated at room temperature for 20 min to allow formation of DNA-PEI complexes. Transfection mixes were subsequently added to cell culture medium and allowed to incubate at 37°C. For stable overexpression, HEK293 Flp-in T-REx stable cell lines were induced to express GFP-LRRK1 or LRRK2 by treatment with 1 µg/ml Doxycycline (Sigma, #D9891) for 24 h. For experiments involving phorbol ester stimulation, cells were incubated in DMEM not containing serum overnight. Cells were then treated with 160 nM phorbol 12-myristate 13-acetate (PMA; Sigma, #P8139) for the time indicated in the figure legends. PMA and kinase inhibitors GÖ6983, CRT0066051 and LXS-196 were all made up in DMSO at a 1000-fold higher concentration than used in cells, which were treated with the indicated doses of inhibitor at 1 : 1000 dilution for the indicated time. An equivalent volume of DMSO was added to cells not treated with an inhibitor or phorbol ester.

Immunoblotting analysis

Lysates were mixed with a quarter of volume or 4× SDS-PAGE sample buffer [50 mM Tris-HCl, pH 6.8, 2% (w/v) SDS, 10% (v/v) glycerol, 0.02% (w/v) Bromophenol Blue and 1% (v/v) 2-mercaptoethanol] (Novex) and heated at 95°C for 5 min. 10–20 µg samples were loaded on to 4–12% NuPAGE™ Bis-Tris gels (Invitrogen, #NP0322BOX) and electrophoresed at 90 V for 15 min, then 150 V for 75 min in NuPAGE™ MOPS buffer (Invitrogen, #NP0001). Proteins were transferred onto nitrocellulose membranes (GE Healthcare, Amersham Protran Supported 0.45 µm, #10600041), at 90 V for 90 min on ice in transfer buffer (48 mM Tris-HCl, 39 mM glycine; freshly supplemented with 20% methanol (v/v)). Transferred membranes were blocked with 5% (w/v) milk in TBST Buffer at room temperature for 60 min. Membranes were then incubated with primary antibodies diluted in blocking buffer overnight at 4°C. After washing membranes in TBST, membranes were incubated at room temperature for 1 h with near-infrared fluorescent IRDye antibodies (LI-COR) diluted 1 : 10 000 in TBST and developed using the LI-COR Odyssey CLx Western Blot imaging system and signal quantified using the Image Studio software. Gathered data was subsequently analysed and plotted in GraphPad Prism (version 9.1.0). The method used for immunoblotting analysis for the LRRK1 pathway further described in detail in a protocols.io method (dx.doi.org/10.17504/protocols.io.6qpvr68e3vmk/v1).

Cloning, expression, and purification of LRRK1 wild type, kinase inactive [D1409A]

Briefly, the DNA coding for the human LRRK1 residues 20 to 2015 (OHu72031 from Genscript) was PCR-amplified using the forward primer TACTTCCAATCCGCTGTGTGTCCAGAACGTGCCATGG and the reverse primer TATCCACCTTTACTGTACCTTCTCTTGGAGTGCAAGCCTCC. The T4 polymerase-treated amplicon was inserted into the transfer vector pFB-6HZB (SGC) by ligation-independent cloning. The respective point mutations were introduced applying the QuikChange method. The resulting plasmids were utilized for the generation of recombinant Baculoviruses according to the Bac-to-Bac expression system protocol (Invitrogen #10359016). Exponentially growing *Spodoptera frugiperda* 9 cells (2×10^6 cells/ml in Lonza Insect-XPRESS medium #BELN12-730Q) were infected with high-titer Baculovirus suspension. After 66 h of incubation (27°C and 90 rpm), cells were harvested by centrifugation. The expressed protein construct contained an N-terminal His6 Z tag, cleavable with TEV protease. For LRRK1 purification, the pelleted *Spodoptera frugiperda* 9 cells were washed with PBS, re-suspended in lysis buffer (50 mM HEPES pH 7.4, 500 mM NaCl, 20 mM imidazole, 0.5 mM TCEP, 5% (v/v) glycerol) and lysed by sonication. The lysate was cleared by centrifugation and loaded onto a Ni NTA column. After vigorous rinsing with lysis buffer the His6-Z tagged protein was eluted in lysis buffer containing 300 mM imidazole. Immediately thereafter, the eluate was diluted with buffer containing no NaCl, to reduce the NaCl-concentration to 250 mM and loaded onto an SP-Sepharose column. His6 Z TEV-LRRK1 was eluted with a 250 mM to 2.5 M NaCl gradient and treated with TEV protease overnight to cleave the His6 Z tag. Contaminating proteins, the cleaved tag, uncleaved protein and TEV protease were removed by another combined SP-Sepharose Ni NTA step. Finally, LRRK1 was concentrated and subjected to gel filtration in storage buffer (20 mM HEPES pH 7.4, 150 mM NaCl, 0.5 mM TCEP, 5% glycerol) using an AKTA Xpress system combined with an S200 gel filtration column. The final yield as calculated from UV absorbance was 0.1 mg/L. The expression method for LRRK1 is further described in a detailed protocols.io method ([dx.doi.org/10.17504/protocols.io.b7ternj](https://doi.org/10.17504/protocols.io.b7ternj)).

Immunofluorescence

For analysis of LRRK1 co-localization with pSer72 Rab7A, PKC α or Na-K ATPase, a freeze-thaw protocol for cell fixation was employed which enables extrusion of cytosolic proteins and enrichment of membrane-associated proteins [49]. Briefly, HEK293 Flp-in T-REx/GFP-LRRK1 cells were seeded at 2.5×10^5 cells/well in six well plates on glass coverslips (VWR, 631-0125; square 22 \times 22 mm thickness 1.5). HEK293 Flp-in T-REx stable cell lines were induced to express GFP-LRRK1 by treatment with 1 μ g/ml Doxycycline for 24 h. For investigation of how LRRK1 phosphosite mutations affect localization, HEK293 wild-type cells were seeded at 2.5×10^5 cells/well in six well plates on glass coverslips. HEK293 cells were then transiently transfected with the indicated GFP-LRRK1 plasmids for 24 h. Subsequently cells were incubated overnight in serum-free media overnight and then treated with 160 nM PMA for a duration of 30 min. Cells were next washed twice with ice-cold PBS buffer (137 mM NaCl, 2.7 mM KCl, 10 mM Na₂HPO₄, 1.8 KH₂PO₄, pH 7.4) and twice with ice-cold glutamate lysis buffer (25 mM HEPES, pH 7.4, 25 mM KCl, 2.5 mM magnesium acetate, 5 mM EGTA, 150 mM potassium glutamate). Coverslips were removed from wells with excess liquid removed by touching the edge on a paper towel. Coverslips were then snap frozen in liquid nitrogen and allowed to thaw at room temperature on a paper towel before replacement into the well. Cells were washed twice with ice-cold glutamate lysis buffer before fixing with 4% (v/v) paraformaldehyde at room temperature for 20 min. Next, unreacted paraformaldehyde was quenched by washing coverslips twice with DMEM (supplemented with 10 mM HEPES, pH 7.4) followed by blocking with 1% (w/v) BSA in PBS for 30 min. The coverslips were incubated with chicken polyclonal anti-GFP (#ab13970, Abcam, Inc.) primary antibody, diluted 1 : 1000 and rabbit monoclonal anti-PKC α (#ab32376, Abcam, Inc.) primary antibody, diluted 1 : 500 or mouse monoclonal anti-Na-K ATPase (#ab76020, Abcam, Inc.) primary antibody, diluted 1 : 500 or rabbit monoclonal anti-pSer72 Rab7A (#302494, Abcam, Inc.) in 1% (w/v) BSA in PBS buffer for 1 h at room temperature followed with three times for 15 min washes with 0.2% (w/v) BSA in PBS. Then the coverslips were incubated with Alexa Fluor® secondary antibody (Invitrogen A-31553) diluted 1 : 500 in 1% (w/v) BSA in PBS for 1 h. The coverslips were washed three times for 15 min with 0.2% (w/v) BSA in PBS and rinsed with distilled water just before mounting. ProLong® Gold Antifade Reagent with DAPI (ThermoFisher, #P36935) was used to mount the coverslips on glass slides (VWR, 631-0117). Slides were then imaged using Leica TCS SP8 MP Multiphoton Microscope using a 40 \times oil immersion lens choosing the optimal imaging resolution with 1-pixel size of 63.3 nm \times 63.3 nm. Images were subsequently analysed using Fiji (<https://fiji.sc/>) and colocalization was quantified using

the Fiji plug-in, JaCoP (<https://imagej.net/plugins/jacop>) which was used to determine Mander's coefficients using automatic thresholds to determine overlap in signal between channels. Coefficients were then statistically analysed in GraphPad Prism (version 9.1.0) using Student's unpaired, two-tailed *t*-tests. This immunofluorescence method is further described in detail in a protocols.io method (dx.doi.org/10.17504/protocols.io.ewov1nmzkgr2/v1).

Membrane fractionation

For crude membrane fractionation, a previously described method was employed [14]. Briefly, 15 cm dishes of HEK293 Flp-in T-REx/GFP-LRRK1 cells were seeded at 1.8×10^7 cells/dish. Cells were then induced to express GFP-LRRK1 by treatment with 1 μ g/ml Doxycycline for 24 h. Subsequently cells were incubated overnight in serum-free media and then treated with 160 nM PMA for a duration of 30 min. Cells were washed twice with ice-cold phosphate buffered saline (PBS; 137 mM NaCl, 2.7 mM KCl, 10 mM Na₂HPO₄ and 1.8 mM KH₂PO₄) resuspended in 400 μ l of a hypotonic solution (10 mM HEPES pH 7.4, 50 mM NaF, 5 mM Sodium Pyrophosphate and complete EDTA-free protease inhibitor cocktail (Roche)). After 15 min of incubation in hypotonic solution, 100 μ l of resuspension buffer (250 mM HEPES, pH 7.4, 750 mM NaCl, 5 mM MgCl₂, 2.5 mM DTT, 500 nM GDP, 250 mM NaF, 25 mM Sodium Pyrophosphate, 1 μ g/ml microcystin-LR and complete EDTA-free protease inhibitor cocktail (Roche)) was added. Cells were homogenized and lysed by passing through a 25-G needle 25 times. Lysates were then centrifuged at 2000g for 5 min at 4°C to pellet nuclei and mitochondrial fraction and the supernatant containing membrane fraction and cytosol was collected. The membrane fraction was then pelleted by ultracentrifugation at 100 000g for 25 min at 4°C. Supernatant which contained the cytoplasmic fraction was collected and carefully transferred into a new tube without disturbing the pellet fraction. Membrane fraction pellet was then washed twice gently with 500 μ l ice cold PBS buffer to remove any cytoplasmic contaminants before being resolubilized in 500 μ l lysis buffer (50 mM HEPES, pH 7.4, 1% (v/v) Triton X-100, 150 mM NaCl, 1 mM MgCl₂, 0.5 mM DTT, 100 nM GDP, 50 mM NaF, 5 mM Sodium Pyrophosphate, 1 μ g/ml microcystin-LR and complete EDTA-free protease inhibitor cocktail (Roche)). Resolubilized membrane fractions were then centrifuged at 2000g for 5 min at 4°C with resultant supernatant containing the solubilized membrane fraction collected into a new tube. The protocol for the membrane fractionation method is further described in detail in a protocols.io method (dx.doi.org/10.17504/protocols.io.yxmvmnb99g3p/v1).

GFP-LRRK1 immunoprecipitation for kinase assay

Briefly, cells were harvested in lysis buffer and clarified by centrifugation at 11 000g for 10 min at 4°C. One thousand micrograms of whole cell lysate was incubated with 10 μ l of packed nanobody anti-GFP binder-Sepharose beads (generated by the MRC PPU Reagents and Services) for 2 h. Bound complexes were recovered by washing the beads twice with 25 mM HEPES pH 7.5, 500 mM NaCl, 10 μ M GTP- γ -S and once with 25 mM HEPES pH 7.5, 150 mM NaCl, 10 μ M GTP- γ -S. Bound complexes were then equilibrated in HEPES kinase buffer (25 mM HEPES, 50 mM KCl and 0.1% (v/v) 2-mercaptoethanol) by washing once. The beads were then directly subjected to a Rab7A kinase assay by incubation in 20 μ l of a mixture containing (1 μ M Rab7A, 1 mM non-radioactive ATP, 10 mM MgAC, 25 mM HEPES, 50 mM KCl and 0.1% (v/v) 2-mercaptoethanol). The reactions were incubated at 30°C for 30 min and terminated by the addition of 20 μ l of 2 \times SDS Sample Buffer containing 1% (v/v) 2-mercaptoethanol. The samples were heated for 10 min at 97°C and the beads separated from the reaction by centrifugation through 0.22 μ m Spin-X columns (CLS8161, Sigma) for 5 min at 3500g. Ten microliters of the resultant sample was analyzed by quantitative immunoblot analysis as described above. The immunoprecipitation kinase assay for GFP-LRRK1 is described in further detail in a protocols.io method (dx.doi.org/10.17504/protocols.io.kqdg3p2wpl25/v1).

Immunoprecipitation and kinase activity for endogenous LRRK1

An amount of 0.5 mg of affinity purified sheep polyclonal total LRRK1 antibody (Sheep number S405C, DU13868) at a concentration of 0.23 mg/ml in PBS buffer was covalently coupled to 25 mg of DynabeadsTM M-270 Epoxy magnetic beads (ThermoFisher, #14302D), according to the manufacturer's protocol. Briefly, the 25 mg of magnetic beads were resuspended in 0.24 ml of C1 Buffer (0.1 M Sodium Phosphate (Na₂HPO₄; NaH₂PO₄) pH 7.4). An amount of 2.4 ml of C2 Buffer (3 M (NH₄)₂SO₄) in 0.1 M Sodium Phosphate pH 7.4) was added. The resulting mixture added to 2.16 ml of the 0.23 mg/ml total LRRK1 antibody and incubated for 16 h at 37°C. The antibody-bead complex was isolated using a magnet separator (DynaMagTM-2, Life Technologies #12321D) and washed in 1 ml of buffer HB (100 mM Glycine pH 11.3), vortexed for 5 s and

immediately washed again in 1 ml of LB Buffer (200 mM Glycine pH 2.8) with 5 s vortexing. This was followed by two washes in 1 ml of SB Buffer (50 mM Tris–HCl pH 7.4, 140 mM NaCl, 0.1% (v/v) Tween-20). The beads were resuspended in 1 ml of SB Buffer and incubated on a roller mixer at room temperature for 10 min. Finally, the coupled antibody-bead complex was isolated and resuspended to give a final concentration of 10 mg of antibody-bead/ml.

For the immunoprecipitations, the equivalent of 2 mg of extracts derived from unstimulated and phorbol ester stimulated wild type and LRRK1 knock-out cells prepared in 0.3% (w/v) CHAPS lysis buffer, were incubated with 50 μ l of the 10 mg/ml antibody-bead complex for 2 h on a shaking platform at 4°C. The antibody-bead complexes were washed twice with 25 mM HEPES pH 7.5, 500 mM NaCl, 10 μ M GTP- γ -S, once with 25 mM HEPES pH 7.5, 150 mM NaCl, 10 μ M GTP- γ -S and finally once in kinase assay buffer (25 mM HEPES, 50 mM KCl and 0.1% (v/v) 2-mercaptoethanol). The beads were subjected to a Rab7A kinase assay as described above. The samples are heated for 10 min at 97°C and removed using a magnet. An amount of 10 μ l of the resultant sample was analysed by quantitative immunoblot analysis as described above.

Phosphorylation and activation of LRRK1 with PKC isoforms

PKC activation kinase assays were conducted in two distinct steps. In the first step, indicated PKC isoforms (100 nM) were incubated with either GFP-LRRK1 immunoprecipitated from 1 mg of HEK293 Flp-in T-REx/GFP-LRRK1 wild-type cell extract or with recombinant LRRK1 (50 nM, residues 20-2015) in a 20 μ l final reaction mixture containing 50 mM HEPES pH 7.5, 0.1% (v/v) 2-mercaptoethanol, 100 μ g/ml L- α -Phosphatidylserine, 10 μ g/ml L- α -Diacylglycerol, 1 mM CaCl₂ and 10 μ M GTP- γ -S, 10 mM MgAc and either 1 mM non-radioactive ATP or where indicated 0.1 mM [γ -³²P]ATP. The reaction mixture was incubated for 30 min at 30°C. In a secondary step, reactions were supplemented with 10 μ l of a master mix containing 1 μ M Rab7A and either 1 mM non-radioactive ATP or when indicated, 0.1 mM [γ -³²P]ATP. The second step of the kinase reaction was carried out at 30°C for the timepoints indicated in the figure legend and reactions terminated by the addition of 10 μ l of 4 \times SDS–PAGE sample buffer containing 1% (v/v) 2-mercaptoethanol. 25% (10 μ l) of total reaction volume was used for each immunoblot analysis. For reactions where [γ -³²P]ATP was employed, 75% (30 μ l) of total reaction volume was analyzed by autoradiography. Briefly, proteins were resolved by SDS–PAGE and detected with Coomassie staining. The gels were imaged with an EPSON scanner, then sandwiched and secured between two sheets of pre-wet cellophane (Bio-Rad) and subsequently dried in a GelAir dryer for 45–60 min. Dried gels were exposed to Amersham Hyperfilm MP overnight (VWR, #28-9068-42), in an autoradiography cassette and the films were later developed using a Konica auto-developer. The method used for activation of LRRK1 by PKC phosphorylation analysis is described in further detail in a protocols.io method (dx.doi.org/10.17504/protocols.io.5jyl89d5rv2w/v1).

Determining stoichiometry of PKC α -mediated LRRK1 phosphorylation

LRRK1 was subjected to PKC α phosphorylation using 0 to 100 nM PKC α as described above using [γ -³²P]ATP of specific activity of ~500 cpm/pmol. Reactions were undertaken in quadruplicate. After polyacrylamide gel electrophoresis the dried Coomassie band corresponding to LRRK1 was excised and ³²P content quantified by Cherenkov counting using liquid scintillation analyzer (TriCarb 4910TR, PerkinElmer). The ratio of ³²P radioactivity/mol of LRRK1 was calculated.

In vitro λ (Lambda) phosphatase treatments

Following immunoprecipitation of GFP-LRRK1 (immunoprecipitated from 1 mg of HEK293 Flp-in T-REx/GFP-LRRK1 WT cell extract), immunoprecipitates are washed once with 500 μ l of 1 \times phosphatase buffer (New England Biolabs, #B7061SVIAL). Washed immunoprecipitates were then incubated with 200 U of λ phosphatase (0.5 μ l of stock 400 000 U/ml) for 30 min at 30°C in a reaction containing 1 \times phosphatase buffer supplemented with 10 mM MnCl₂. For the inactivated phosphatase controls, λ phosphatase activity was inhibited by pre-incubation of λ phosphatase with 50 mM EDTA for 10 min to enable complete inhibition prior to addition to immunoprecipitates.

Phosphosite identification by mass spectrometry

A 20 μ l reaction mixture was set up containing 200 nM of kinase inactive LRRK1[D1409A, 20-2015] (1 μ g), 400 nM recombinant full-length PKC α (500 ng) in a buffer containing 50 mM HEPES pH 7.5, 0.1% (v/v) 2-mercaptoethanol, 100 μ g/ml L- α -Phosphatidylserine, 10 μ g/ml L- α -Diacylglycerol, 1 mM CaCl₂ and 10 μ M

GTP- γ -S, 10 mM MgAc and 1 mM ATP (non-radioactive) for 30 min at 30°C. The reactions were stopped by the addition of 6.6 μ l of 4 \times SDS–PAGE sample buffer containing 1% (v/v) 2-mercaptoethanol, and samples subjected to electrophoresis on a 4–12% SDS–PAGE gels. The gel was stained with Coomassie blue and the bands corresponding to LRRK1 were excised and destained by three 10 min washes in 40% (v/v) acetonitrile in 40 mM NH₄HCO₃. Gel pieces were then reduced by incubation in 5 mM DTT in 40 mM NH₄HCO₃ at 56°C for 30 min. The DTT solution was removed by careful pipetting and washed in 40% (v/v) acetonitrile in 40 mM NH₄HCO₃ for 10 min. This was followed by alkylation of the samples by addition of 20 mM iodoacetamide in 40 mM NH₄HCO₃ for 20 min at room temperature. Gel pieces were subsequently dehydrated by washing in 100% (v/v) acetonitrile for 10 min. Acetonitrile is removed by careful pipetting and vacuum drying for 10 min to remove any residual acetonitrile. Proteases (w/v) were freshly prepared in the appropriate buffers (Trypsin + LysC in 50 mM TEABC, Asp-N in 50 mM Tris–HCl, Chymotrypsin in 100 mM Tris–HCl + 10 mM CaCl₂) and 100 ng of proteases were added to gel pieces and incubated overnight on a thermomixer at 37°C, 800 \times g. Digested peptides were extracted from gel pieces by addition of 200 μ l of extraction buffer (80% (v/v) acetonitrile in 0.2% (v/v) formic Acid), incubated on a Thermomixer with an agitation at 800 \times g for 20 min. The extraction was completed by repeating this step again. The eluate was immediately vacuum dried and resuspended in 80 μ l of Solution A (0.1% (v/v) TFA (trifluoroacetic acid)). Resuspended peptides were then subjected to a C18 clean-up using in-house prepared C18 stage tips. One C18 disk was prepared by punching with 16-gauge needle and loaded on to 250 μ l pipette tips. C18 resin was activated by addition of 100 μ l of acetonitrile and centrifuged for 2 min at 2000 \times g. Flow through was discarded and C18 resin was equilibrated by addition of 80 μ l of Solution A (0.1% (v/v) TFA) and centrifuged for 2 min at 2000 \times g. Flow through were discarded again and peptide digests were loaded onto C18 resin and centrifuged at 1500 \times g for 5 min. The flow through was re-applied and subsequently centrifuged at 1500 \times g for 5 min. C18 resins were then washed twice by addition of 80 μ l of Solution A (0.1% (v/v) TFA) and centrifuged for 2 min at 2000 \times g. Peptides were eluted by addition of 80 μ l of Solution B (40% (v/v) acetonitrile in 0.1% (v/v) TFA) and centrifuged for 2 min at 1500 \times g. Eluates were immediately snap frozen and vacuum dried completely. A further detailed description of *in vitro* phosphosite identification method has been published on protocols.io ([dx.doi.org/10.17504/protocols.io.261gen89dg47/v1](https://doi.org/10.17504/protocols.io.261gen89dg47/v1)).

LC–MS/MS and data analysis

Vacuum dried peptides of each sample was resolubilized in LC-buffer (3% (v/v) acetonitrile in 0.1% (v/v) formic acid) and incubated on a Thermo mixer at 1800 rpm at room temperature for 30 min. Furthermore, 200 ng of peptide digest was loaded onto Evotips and samples were prepared as explained in [50]. The Evotips were further placed on an autosampler tray of EvoSep LC system for LC–MS/MS analysis. Thirty samples per day (44 min run time) method was used and the peptides were resolved on a 15 cm analytical column (ReproSil–Pur C18, 1.9 μ m beads by Dr Maisch. #EV1113) and directly electrosprayed using Easy nano LC source into the Orbitrap Exploris 240 (Thermo Fisher Scientific) mass spectrometer. The data was acquired in a Data dependent mode (DDA) targeting top-10 dependent scans. The full MS and MS2 scans were acquired at 120 000 and 15 000 resolution (m/z 200), respectively, and measured using Orbitrap mass analyzer. The precursor ions were fragmented using 28% normalized Higher-energy collisional dissociation (HCD). The AGC target for MS1 and MS2 are set at 3×10^6 and 1×10^5 ions respectively and maximum ion injection times were set for MS1 and MS2 are 25 and 100 ms. The dynamic exclusion option was enabled and was set for 5 s durations.

Database searches

The MS raw data was processed using MaxQuant software suite version 2.0.3.0 [51]. Human LRRK1 sequence from Uniprot was used as a FASTA sequence to search the data. Trypsin + Lys-C, AspN and Chymotrypsin were set as proteases with a maximum of two missed cleavages were allowed. Oxidation of Met, deamidation of Asn/Gln and phosphorylation of Ser/Thr were set as a variable modification and Carbamidomethylation of Cys was set as a fixed modification. The default instrument parameters for MS1 and MS2 tolerance were used, and the data was filtered for 1% PSM, peptide and Protein level FDR. The pSTY sites table was further processed using in-house python script (<https://zenodo.org/record/6627264>) to generate the heatmap representation of identified high-confident LRRK1 phosphosites.

LCMS analysis of LRRK1 digests using ZenoTOF 7600

LRRK1 tryptic digests were analyzed using a Waters M Class UPLC system coupled to ZenoTOF 7600 mass spectrometer (Sciex). Digests were chromatographed on a Kinetix XB C18 150 × 0.3 mm column (Phenomenex) at 6 ml/min (A = 0.1% Formic acid in water, B = 0.1% formic acid in acetonitrile) with a 21 min gradient (3–30% B) followed by 3 min (30–80% B). The column was connected directly to the ZenoTOF 7600 Optiflow™ source fitted with a low microflow probe and heated at 30°C with the integral column oven.

LCMS data was acquired using optimal source conditions and the data dependent acquisition was performed on the Top 30 precursors (m/z 400–2000) with charge state 2–4+, with a minimum intensity of 300 cps and excluded for 6 sec after one occurrence. TOFMSMS spectra (m/z 100–2000) were acquired with Electron Activated Dissociation (EAD) using a filament current of 3000 nA, 0 eV kinetic energy, a reaction time of 10 ms and total MSMS accumulation time of 15 ms. Data files (wiff) were converted to mgf files using the AB Sciex MS Data converter (Sciex) and searched using Mascot 2.6 against Swissprot (2019_11.fasta) database. Enzyme cleavage allowed for one missed cleavage, Carbamidomethylation of cysteine was a fixed modification, phosphorylation of serine, threonine, tyrosine, and oxidation of methionine were variable modifications. The instrument type chosen to match the EAD spectra was EThcD and the mass accuracy for precursors (20 ppm) and for MSMS spectra (0.05 Da).

Data Availability

All the primary data that is presented in this study has been deposited in Zenodo and repository and can be accessed using the Digital Object Identifier 10.5281/zenodo.6974577. The mass spectrometry proteomics data have been deposited to the ProteomeXchange Consortium via the PRIDE [52] partner repository with the dataset identifier PXD034420. All reagents (and associated datasheets) generated at the MRC Protein Phosphorylation and Ubiquitylation Unit at the University of Dundee can be requested using the indicated DU number identifier through our reagent's website <https://mrcppureagents.dundee.ac.uk/>.

Competing Interests

The authors declare that there are no competing interests associated with the manuscript.

Funding

D.R.A and S.K. laboratories are funded by the joint efforts of The Michael J. Fox Foundation for Parkinson's Research (MJFF) and Aligning Science Across Parkinson's (ASAP) initiative. MJFF administers the grant (ASAP-000463-D.R.A. and ASAP-000159-S.K.) on behalf of ASAP and itself. The D.R.A lab is also supported by the UK Medical Research Council [grant number MC_UU_00018/1] and the pharmaceutical companies supporting the Division of Signal Transduction Therapy Unit (Boehringer Ingelheim, GlaxoSmithKline, Merck KGaA.).

Open Access

Open access for this article was enabled by the participation of University of Dundee in an all-inclusive *Read & Publish* agreement with Portland Press and the Biochemical Society under a transformative agreement with JISC.

CRedit Author Contribution

Dario R. Alessi: Conceptualization, Resources, Formal analysis, Supervision, Funding acquisition, Methodology, Writing — original draft, Project administration, Writing — review and editing. **Asad U. Malik:** Conceptualization, Resources, Formal analysis, Validation, Investigation, Methodology, Writing — original draft, Writing — review and editing. **Athanasios Karapetsas:** Conceptualization, Resources, Formal analysis, Validation, Investigation, Methodology, Writing — original draft, Writing — review and editing. **Raja S. Nirujogi:** Conceptualization, Resources, Formal analysis, Validation, Investigation, Visualization, Methodology, Writing — original draft, Writing — review and editing. **Deep Chatterjee:** Resources, Investigation, Methodology. **Toan K. Phung:** Software, Formal analysis, Methodology. **Melanie Wightman:** Resources, Methodology. **Robert Gourlay:** Formal analysis, Methodology. **Nicholas A. Morrice:** Resources, Formal analysis, Investigation, Visualization, Methodology. **Sebastian Mathea:** Resources, Formal analysis, Supervision, Funding acquisition, Methodology. **Stefan Knapp:** Resources, Formal analysis, Supervision, Funding acquisition, Methodology.

Acknowledgements

We thank Nicole Polinski at the Michael J Fox Foundation for Parkinson's research for coordinating the generation of the rabbit monoclonal pRab7A Ser72 antibody that made this study possible, and Suzanne Pfeffer (Stanford), Samara Reck-Peterson, Andres Leschziner (UCSD) and Ji Sun (St Jude) for helpful discussions. We also thank the excellent technical support of the MRC protein phosphorylation and ubiquitylation unit (PPU) DNA sequencing service (coordinated by Gary Hunter), the MRC-PPU tissue culture team (coordinated by Edwin Allen), MRC-PPU Reagents and Services cloning team (coordinated by Dr Rachel Toth), antibody and protein purification teams (coordinated by Dr James Hastie), and mass spectrometry team (coordinated by Dr Renata Filipe Soares). For the purpose of open access, the authors have applied a CC BY public copyright license to all Author Accepted Manuscripts arising from this submission.

Abbreviations

EAD, electron activated dissociation; HCD, higher energy collisional dissociation; LRRK1, Leucine-rich-repeat-kinase 1; MEFs, mouse embryonic fibroblasts; PKC, Protein Kinase C; PMA, Phorbol 12-myristate 13-acetate; TFA, trifluoroacetic acid.

References

- 1 Sejwal, K., Chami, M., Rémigny, H., Vancraenenbroeck, R., Sibrán, W., Sütterlin, R. et al. (2017) Cryo-EM analysis of homodimeric full-length LRRK2 and LRRK1 protein complexes. *Sci. Rep.* **7**, 8667 <https://doi.org/10.1038/s41598-017-09126-z>
- 2 Snead, D.M., Matyszewski, M., Dickey, A.M., Lin, Y.X., Leschziner, A.E. and Reck-Peterson, S.L. (2022) Structural basis for Parkinson's disease-linked LRRK2's binding to microtubules. *bioRxiv* <https://doi.org/10.1101/2022.01.21.477284>
- 3 Xing, W.R., Goodluck, H., Zeng, C. and Mohan, S. (2017) Role and mechanism of action of leucine-rich repeat kinase 1 in bone. *Bone Res.* **5**, 17003 <https://doi.org/10.1038/boneres.2017.3>
- 4 Guo, L., Girisha, K.M., Iida, A., Hebbar, M., Shukla, A., Shah, H. et al. (2017) Identification of a novel LRRK1 mutation in a family with osteosclerotic metaphyseal dysplasia. *J. Hum. Genet.* **62**, 437–441 <https://doi.org/10.1038/jhg.2016.136>
- 5 Zimprich, A., Benet-Pages, A., Struhal, W., Graf, E., Eck, S.H., Offman, M.N. et al. (2011) A mutation in VPS35, encoding a subunit of the retromer complex, causes late-onset Parkinson disease. *Am. J. Hum. Genet.* **89**, 168–175 <https://doi.org/10.1016/j.ajhg.2011.06.008>
- 6 Paisan-Ruiz, C., Jain, S., Evans, E.W., Gilks, W.P., Simon, J., van der Brug, M. et al. (2004) Cloning of the gene containing mutations that cause PARK8-linked Parkinson's disease. *Neuron* **44**, 595–600 <https://doi.org/10.1016/j.neuron.2004.10.023>
- 7 Hanafusa, H., Yagi, T., Ikeda, H., Hisamoto, N., Nishioka, T., Kaibuchi, K. et al. (2019) LRRK1 phosphorylation of Rab7 at S72 links trafficking of EGFR-containing endosomes to its effector RILP. *J. Cell Sci.* **132**, jcs228809 <https://doi.org/10.1242/jcs.228809>
- 8 Malik, A.U., Karapetsas, A., Nirujogi, R.S., Mathea, S., Chatterjee, D., Pal, P. et al. (2021) Deciphering the LRRK code: LRRK1 and LRRK2 phosphorylate distinct Rab proteins and are regulated by diverse mechanisms. *Biochem. J.* **478**, 553–578 <https://doi.org/10.1042/BCJ20200937>
- 9 Steger, M., Tonelli, F., Ito, G., Davies, P., Trost, M., Vetter, M. et al. (2016) Phosphoproteomics reveals that Parkinson's disease kinase LRRK2 regulates a subset of Rab GTPases. *eLife* **5**, e12813 <https://doi.org/10.7554/eLife.12813>
- 10 Steger, M., Diez, F., Dhekne, H.S., Lis, P., Nirujogi, R.S., Karayel, O. et al. (2017) Systematic proteomic analysis of LRRK2-mediated Rab GTPase phosphorylation establishes a connection to ciliogenesis. *eLife* **6**, e31012 <https://doi.org/10.7554/eLife.31012>
- 11 Waschbüsch, D., Purlyte, E., Pal, P., McGrath, E., Alessi, D.R. and Khan, A.R. (2020) Structural basis for Rab8a recruitment of RILPL2 via LRRK2 phosphorylation of switch 2. *Structure* **28**, 406–417.e406 <https://doi.org/10.1016/j.str.2020.01.005>
- 12 Bonet-Ponce, L., Beilina, A., Williamson, C.D., Lindberg, E., Kluss, J.H., Saez-Atienzar, S. et al. (2020) LRRK2 mediates tubulation and vesicle sorting from lysosomes. *Sci. Adv.* **6**, eabb2454 <https://doi.org/10.1126/sciadv.abb2454>
- 13 Dhekne, H.S., Yanatori, I., Vides, E.G., Sobu, Y., Diez, F., Tonelli, F. et al. (2021) LRRK2-phosphorylated rab10 sequesters myosin Va with RILPL2 during ciliogenesis blockade. *Life Sci. Alliance* **4**, e202101050 <https://doi.org/10.26508/lsa.202101050>
- 14 Purlyte, E., Dhekne, H.S., Sarhan, A.R., Gomez, R., Lis, P., Wightman, M. et al. (2018) Rab29 activation of the Parkinson's disease-associated LRRK2 kinase. *EMBO J.* **37**, 1–18 <https://doi.org/10.15252/embj.201798099>
- 15 Liu, Z., Bryant, N., Kumaran, R., Beilina, A., Abeliovich, A., Cookson, M.R. et al. (2018) LRRK2 phosphorylates membrane-bound Rabs and is activated by GTP-bound Rab7L1 to promote recruitment to the trans-Golgi network. *Hum. Mol. Genet.* **27**, 385–395 <https://doi.org/10.1093/hmg/ddx410>
- 16 Gomez, R.C., Wawro, P., Lis, P., Alessi, D.R. and Pfeffer, S.R. (2019) Membrane association but not identity is required for LRRK2 activation and phosphorylation of Rab GTPases. *J. Cell Biol.* **218**, 4157–4170 <https://doi.org/10.1083/jcb.201902184>
- 17 Vides, E.G., Adhikari, A., Lis, P., Purlyte, E., Shumate, J., Lasso, E.S. et al. (2022) A feed-forward pathway drives LRRK2 kinase membrane recruitment and apparent activation. *bioRxiv* <https://doi.org/10.1101/2022.04.25.489459>
- 18 Zhu, H., Tonelli, F., Alessi, D.R. and Sun, J. (2022) Structural basis of human LRRK2 membrane recruitment and activation. *bioRxiv* <https://doi.org/10.1101/2022.04.26.489605>
- 19 Mir, R., Tonelli, F., Lis, P., Macartney, T., Polinski, N.K., Martinez, T.N. et al. (2018) The Parkinson's disease VPS35[D620N] mutation enhances LRRK2-mediated Rab protein phosphorylation in mouse and human. *Biochem. J.* **475**, 1861–1883 <https://doi.org/10.1042/BCJ20180248>
- 20 Mellor, H. and Parker, P.J. (1998) The extended protein kinase C superfamily. *Biochem. J.* **332**, 281–292 <https://doi.org/10.1042/bj3320281>
- 21 Edwards, A.S., Faux, M.C., Scott, J.D. and Newton, A.C. (1999) Carboxyl-terminal phosphorylation regulates the function and subcellular localization of protein kinase C betaII. *J. Biol. Chem.* **274**, 6461–6468 <https://doi.org/10.1074/jbc.274.10.6461>
- 22 Le Good, J.A., Ziegler, W.H., Parekh, D.B., Alessi, D.R., Cohen, P. and Parker, P.J. (1998) Protein kinase C isoforms controlled by phosphoinositide 3-kinase through the protein kinase PDK1. *Science* **281**, 2042–2045 <https://doi.org/10.1126/science.281.5385.2042>

- 23 Dutil, E.M., Toker, A. and Newton, A.C. (1998) Regulation of conventional protein kinase C isozymes by phosphoinositide-dependent kinase 1 (PDK-1). *Curr. Biol.* **8**, 1366–1375 [https://doi.org/10.1016/S0960-9822\(98\)00017-7](https://doi.org/10.1016/S0960-9822(98)00017-7)
- 24 Baffi, T.R., Lorden, G., Wozniak, J.M., Feichtner, A., Yeung, W., Kornev, A.P. et al. (2021) mTORC2 controls the activity of PKC and Akt by phosphorylating a conserved TOR interaction motif. *Sci. Signal.* **14**, eabe4509 <https://doi.org/10.1126/scisignal.abe4509>
- 25 Liu, W.S. and Heckman, C.A. (1998) The sevenfold way of PKC regulation. *Cell Signal.* **10**, 529–542 [https://doi.org/10.1016/S0898-6568\(98\)00012-6](https://doi.org/10.1016/S0898-6568(98)00012-6)
- 26 Chou, M.M., Hou, W., Johnson, J., Graham, L.K., Lee, M.H., Chen, C.S. et al. (1998) Regulation of protein kinase C zeta by PI 3-kinase and PDK-1. *Curr. Biol.* **8**, 1069–1077 [https://doi.org/10.1016/S0960-9822\(98\)70444-0](https://doi.org/10.1016/S0960-9822(98)70444-0)
- 27 Balendran, A., Hare, G.R., Kieloch, A., Williams, M.R. and Alessi, D.R. (2000) Further evidence that 3-phosphoinositide-dependent protein kinase-1 (PDK1) is required for the stability and phosphorylation of protein kinase C (PKC) isoforms. *FEBS Lett.* **484**, 217–223 [https://doi.org/10.1016/S0014-5793\(00\)02162-1](https://doi.org/10.1016/S0014-5793(00)02162-1)
- 28 Moscat, J. and Diaz-Meco, M.T. (2000) The atypical protein kinase Cs. functional specificity mediated by specific protein adaptors. *EMBO Rep.* **1**, 399–403 <https://doi.org/10.1093/embo-reports/kvd098>
- 29 Nishikawa, K., Toker, A., Johannes, F.J., Songyang, Z. and Cantley, L.C. (1997) Determination of the specific substrate sequence motifs of protein kinase C isozymes. *J. Biol. Chem.* **272**, 952–960 <https://doi.org/10.1074/jbc.272.2.952>
- 30 Kang, J.H., Toita, R., Kim, C.W. and Katayama, Y. (2012) Protein kinase C (PKC) isozyme-specific substrates and their design. *Biotechnol. Adv.* **30**, 1662–1672 <https://doi.org/10.1016/j.biotechadv.2012.07.004>
- 31 Zugaza, J.L., Sinnott-Smith, J., Van Lint, J. and Rozengurt, E. (1996) Protein kinase D (PKD) activation in intact cells through a protein kinase C-dependent signal transduction pathway. *EMBO J.* **15**, 6220–6230 <https://doi.org/10.1002/j.1460-2075.1996.tb01012.x>
- 32 Gschwendt, M., Dieterich, S., Rennecke, J., Kittstein, W., Mueller, H.J. and Johannes, F.J. (1996) Inhibition of protein kinase C mu by various inhibitors. differentiation from protein kinase c isoenzymes. *FEBS Lett.* **392**, 77–80 [https://doi.org/10.1016/0014-5793\(96\)00785-5](https://doi.org/10.1016/0014-5793(96)00785-5)
- 33 Zhang, H., Zha, X., Tan, Y., Hornbeck, P.V., Mastrangelo, A.J., Alessi, D.R. et al. (2002) Phosphoprotein analysis using antibodies broadly reactive against phosphorylated motifs. *J. Biol. Chem.* **277**, 39379–39387 <https://doi.org/10.1074/jbc.M206399200>
- 34 Schonwasser, D.C., Marais, R.M., Marshall, C.J. and Parker, P.J. (1998) Activation of the mitogen-activated protein kinase/extracellular signal-regulated kinase pathway by conventional, novel, and atypical protein kinase C isotypes. *Mol. Cell. Biol.* **18**, 790–798 <https://doi.org/10.1128/MCB.18.2.790>
- 35 Kraft, A.S., Smith, J.B. and Berkow, R.L. (1986) Bryostatin, an activator of the calcium phospholipid-dependent protein kinase, blocks phorbol ester-induced differentiation of human promyelocytic leukemia cells HL-60. *Proc. Natl Acad. Sci. U.S.A.* **83**, 1334–1338 <https://doi.org/10.1073/pnas.83.5.1334>
- 36 Zhang, F.L. and Casey, P.J. (1996) Protein prenylation: molecular mechanisms and functional consequences. *Annu. Rev. Biochem.* **65**, 241–269 <https://doi.org/10.1146/annurev.bi.65.070196.001325>
- 37 Luzzio, M., Papillon, J. and Visser, M.S. (2018) Protein kinase C inhibitors and methods of their use United States Patent Application. 20180179181, Application Number 15/830769
- 38 Arang, N., C., M., Rigracciolo, D.R., Lubrano, S., Saddawi-Konefka, R., Wang, Z. et al. (2022) High throughput chemogenetic drug screening reveals kinase-driven therapeutic vulnerabilities in GNAQ-mutant uveal melanoma. In Preparation
- 39 Alessi, D.R. (1997) The protein kinase C inhibitors Ro 318220 and GF 109203X are equally potent inhibitors of MAPKAP kinase-1beta (Rsk-2) and p70 S6 kinase. *FEBS Lett.* **402**, 121–123 [https://doi.org/10.1016/S0014-5793\(96\)01510-4](https://doi.org/10.1016/S0014-5793(96)01510-4)
- 40 Hutti, J.E., Jarrell, E.T., Chang, J.D., Abbott, D.W., Storz, P., Toker, A. et al. (2004) A rapid method for determining protein kinase phosphorylation specificity. *Nat. Methods* **1**, 27–29 <https://doi.org/10.1038/nmeth708>
- 41 Evans, I.M., Bagherzadeh, A., Charles, M., Raynham, T., Ireson, C., Boakes, A. et al. (2010) Characterization of the biological effects of a novel protein kinase D inhibitor in endothelial cells. *Biochem. J.* **429**, 565–572 <https://doi.org/10.1042/BJ20100578>
- 42 Cohen, P.T. and Cohen, P. (1989) Discovery of a protein phosphatase activity encoded in the genome of bacteriophage lambda. probable identity with open reading frame 221. *Biochem. J.* **260**, 931–934 <https://doi.org/10.1042/bj2600931>
- 43 Reyniers, L., Del Giudice, M.G., Civiero, L., Belluzzi, E., Lobbstaël, E., Beilina, A. et al. (2014) Differential protein-protein interactions of LRRK1 and LRRK2 indicate roles in distinct cellular signaling pathways. *J. Neurochem.* **131**, 239–250
- 44 Taylor, S.S. and Kornev, A.P. (2011) Protein kinases: evolution of dynamic regulatory proteins. *Trends Biochem. Sci.* **36**, 65–77 <https://doi.org/10.1016/j.tibs.2010.09.006>
- 45 Jumper, J., Evans, R., Pritzel, A., Green, T., Figurnov, M., Ronneberger, O. et al. (2021) Highly accurate protein structure prediction with alphaFold. *Nature* **596**, 583–589 <https://doi.org/10.1038/s41586-021-03819-2>
- 46 Weng, J.H., Aoto, P.C., Lorenz, R., Wu, J., Schmidt, S.H., Manschwetus, J.T. et al. (2022) LRRK2 dynamics analysis identifies allosteric control of the crossstalk between its catalytic domains. *PLoS Biol.* **20**, e3001427 <https://doi.org/10.1371/journal.pbio.3001427>
- 47 Lis, P., Burel, S., Steger, M., Mann, M., Brown, F., Diez, F. et al. (2018) Development of phospho-specific Rab protein antibodies to monitor in vivo activity of the LRRK2 Parkinson's disease kinase. *Biochem. J.* **475**, 1–22 <https://doi.org/10.1042/BCJ20170802>
- 48 Reed, S.E., Staley, E.M., Mayginnes, J.P., Pintel, D.J. and Tullis, G.E. (2006) Transfection of mammalian cells using linear polyethylenimine is a simple and effective means of producing recombinant adeno-associated virus vectors. *J. Virol. Methods* **138**, 85–98 <https://doi.org/10.1016/j.jviromet.2006.07.024>
- 49 Seaman, M.N. (2004) Cargo-selective endosomal sorting for retrieval to the Golgi requires retromer. *J. Cell Biol.* **165**, 111–122 <https://doi.org/10.1083/jcb.200312034>
- 50 Nirujogi, R.S., Tonelli, F., Taylor, M., Lis, P., Zimprich, A., Sammler, E. et al. (2021) Development of a multiplexed targeted mass spectrometry assay for LRRK2-phosphorylated rabs and Ser910/Ser935 biomarker sites. *Biochem. J.* **478**, 299–326 <https://doi.org/10.1042/BCJ20200930>
- 51 Cox, J. and Mann, M. (2008) Maxquant enables high peptide identification rates, individualized p.p.b.-range mass accuracies and proteome-wide protein quantification. *Nat. Biotechnol.* **26**, 1367–1372 <https://doi.org/10.1038/nbt.1511>
- 52 Perez-Riverol, Y., Bai, J., Bandla, C., Garcia-Seisdedos, D., Hewapathirana, S., Kamatchinathan, S. et al. (2022) The PRIDE database resources in 2022: a hub for mass spectrometry-based proteomics evidences. *Nucleic Acids Res.* **50**, D543–D552 <https://doi.org/10.1093/nar/gkab1038>
- 53 Ashkenazy, H., Abadi, S., Martz, E., Chay, O., Mayrose, I., Pupko, T. et al. (2016) ConSurf 2016: an improved methodology to estimate and visualize evolutionary conservation in macromolecules. *Nucleic Acids Res.* **44**, W344–W350 <https://doi.org/10.1093/nar/gkw408>

- 54 Kriventseva, E.V., Kuznetsov, D., Tegenfeldt, F., Manni, M., Dias, R., Simao, F.A. et al. (2019) OrthoDB v10: sampling the diversity of animal, plant, fungal, protist, bacterial and viral genomes for evolutionary and functional annotations of orthologs. *Nucleic Acids Res.* **47**, D807–D811 <https://doi.org/10.1093/nar/gky1053>
- 55 Katoh, K. and Standley, D.M. (2013) MAFFT multiple sequence alignment software version 7: improvements in performance and usability. *Mol. Biol. Evol.* **30**, 772–780 <https://doi.org/10.1093/molbev/mst010>
- 56 Herbst, S., Campbell, P., Harvey, J., Bernard, E.M., Papayannopoulos, V., Wood, N.W. et al. (2020) LRRK2 activation controls the repair of damaged endomembranes in macrophages. *EMBO J.* **39**, e104494 <https://doi.org/10.15252/emj.2020104494>
- 57 Kuwahara, T., Funakawa, K., Komori, T., Sakurai, M., Yoshii, G., Eguchi, T. et al. (2020) Roles of lysosomotropic agents on LRRK2 activation and Rab10 phosphorylation. *Neurobiol. Dis.* **145**, 105081 <https://doi.org/10.1016/j.nbd.2020.105081>
- 58 Kalogeropoulou, A.F., Freemantle, J.B., Lis, P., Vides, E.G. Polinski, N.K. and Alessi, D.R. (2020) Endogenous Rab29 does not impact basal or stimulated LRRK2 pathway activity. *Biochem. J.* **477**, 4397–4423 <https://doi.org/10.1042/BCJ20200458>